HHS Public Access

Author manuscript

Cell Biochem Biophys. Author manuscript; available in PMC 2022 May 24.

Published in final edited form as:

Cell Biochem Biophys. 2021 September ; 79(3): 575–592. doi:10.1007/s12013-021-01005-9.

Nuclear Sphingosine-1-phosphate Lyase Generated Δ2-hexadecenal is A Regulator of HDAC Activity and Chromatin Remodeling in Lung Epithelial Cells

David L. Ebenezer[1], **Ramaswamy Ramchandran**[1], **Panfeng Fu**[2], **Lizar A. Mangio**[1], **Vidyani Suryadevara**[1], **Alison W. Ha**[3], **Evgeny Berdyshev**[4], **Paul P. Van Veldhoven**[5], **Stephen J. Kron**[6], **Fabian Schumacher**[7], **Burkhard Kleuser**[7], **Viswanathan Natarajan**[1,8]

[1]Departments of Pharmacology & Regenerative Medicine, University of Illinois at Chicago, Chicago, IL, USA

[2]The Affiliated Hospital of School of Medicine, Ningbo University, Ningbo, China

[3]Department of Biochemistry & Molecular Genetics, University of Illinois at Chicago, Chicago, IL, USA

[4]Department of Medicine, National Jewish Medical Center, Denver, CO, USA

[5]LIPIT, Department of Cellular and Molecular Medicine, KU Leuven, Leuven, Belgium

[6]Department of Molecular Genetics and Cell Biology and Ludwig Center for Metastasis Research, The University of Chicago, Chicago, IL, USA

[7]Institute of Pharmacy, Department of Pharmacology & Toxicology, Freie Universität Berlin, Berlin, Germany

[8]Department of Medicine, University of Illinois at Chicago, Chicago, IL, USA

Abstract

Sphingosine-1-phosphate (S1P), a bioactive lipid mediator, is generated from sphingosine by sphingosine kinases (SPHKs) 1 and 2 and is metabolized to Δ2-hexadecenal (Δ2-HDE) and ethanolamine phosphate by S1P lyase (S1PL) in mammalian cells. We have recently demonstrated the activation of nuclear SPHK2 and the generation of S1P in the nucleus of lung epithelial cells exposed to *Pseudomonas aeruginosa*. Here, we have investigated the nuclear localization of S1PL and the role of *Δ*2-HDE generated from S1P in the nucleus as a modulator of histone deacetylase (HDAC) activity and histone acetylation. Electron micrographs of the nuclear fractions isolated from MLE-12 cells showed nuclei free of ER contamination, and S1PL activity was detected in nuclear fractions isolated from primary lung bronchial epithelial cells and alveolar epithelial MLE-12 cells. *Pseudomonas aeruginosa*-mediated nuclear Δ2-HDE generation, and H3/H4 histone

✉Viswanathan Natarajan, visnatar@uic.edu.

Authors' Contributions Conceptualization—D.L.E., V.N., and B.K.; Methodology—D.L.E., R.R., P.F.U., V.N., A.W.H., L.A.M., P.P.K.K., E.V.B., and F.S.; Formal analysis—D.L.E., P.P.K.K., R.R., E.V.B., and V.N.; Investigation—D.L.E., V.N., B.K., and F.S.; Resources—V.N., B.K., P.P.V.V., and S.J.K.; Writing (Review and editing)—R.R. and V.N.; Project administration—V.N.; Funding acquisition—V.N. and S.J.K.

Conflict of Interest The authors declare no competing interests.

acetylation was attenuated by S1PL inhibitors in MLE-12 cells and human bronchial epithelial cells. In vitro, the addition of exogenous Δ2-HDE (100–10,000 nM) to lung epithelial cell nuclear preparations inhibited HDAC1/2 activity, and increased acetylation of Histone H3 and H4, whereas similar concentrations of S1P did not show a significant change. In addition, incubation of Δ2-HDE with rHDAC1 generated five different amino acid adducts as detected by LC-MS/MS; the predominant adduct being Δ2-HDE with lysine residues of HDAC1. Together, these data show an important role for the nuclear S1PL-derived Δ2-HDE in the modification of HDAC activity, histone acetylation, and chromatin remodeling in lung epithelial cells.

Keywords

S1P lyase; Hexadecenal; Nuclear S1P; HDAC1/2; Histone acetylation; Pseudomonas-induced lung inflammation

Introduction

Sphingosine-1-phosphate (S1P), the simplest sphingophospholipid in the human sphingolipidome, is biosynthesized by phosphorylation of sphingosine (Sph), catalyzed by sphingosine kinases (SPHKs) 1 and 2 [1–3]. The subcellular distribution of SPHK1 and SPHK2 varies in different cell types which dictate the spatio-temporal S1P production and function [4, 5]. Intracellular S1P levels in most of the mammalian cells, except erythrocytes and platelets, are lower compared to plasma [6, 7] as S1P is metabolized by S1P phosphatases 1 and 2 [8] and lipid phosphate phosphatases [9, 10] to Sph, and by S1P lyase to Δ2-hexadecenal (Δ2-HDE) and ethanolamine phosphate [11]. In addition, S1P lyase also hydrolyzes dihydro S1P to hexadecanal and ethanolamine phosphate. S1P lyase is a pyridoxal phosphate-dependent enzyme that is predominantly localized in the endoplasmic reticulum (ER) [12]; however, its presence in the nucleus has not been carefully investigated.

Recent advances in lipidomics by LC-MS/MS reveal S1P to be a constituent of nuclear lipids. Nuclear S1P levels in epithelial cells (<10 pmoles/mg protein) [13, 14] and breast cancer cell line MCF-7 (~2 pmol) [15] are much lower compared to the levels of sph and ceramide. Further, infection of lung epithelial cells with *Pseudomonas aeruginosa* (*P. aeruginosa*) [14] or ecto-expression of SPHK2 in MCF-7 cells [16] enhanced nuclear S1P levels. Similarly, the treatment of mouse embryonic fibroblasts with FTY720, an analog of Sph, increased the accumulation of FTY720-P in the nuclear fraction [16]. A key step in nuclear S1P generation is the phosphorylation and nuclear localization of SPHK2, and SPHK2, but not SPHK1, possesses nuclear import, and export sequences [17]. Stimulation of MCF-7 cells with phorbol myristate acetate [14], or in vivo infection of mouse lung or in vitro challenge of lung epithelial cells with *P.* aeruginosa-induced SPHK2 phosphorylation, and its nuclear localization [14]. Inhibition of SPHK2 activity with a SPHK2 inhibitor ABC294640 reduced *P.* aeruginosa-mediated nuclear S1P production, suggesting a potential role for nuclear SPHK2 in cell function [14].

The role of nuclear S1P breakdown products has not yet been fully defined. Our initial studies showed the presence of Δ2-HDE in nuclear lipid extracts of unstimulated lung alveolar epithelial cells, and treatment with *P. aeruginosa* increased nuclear Δ2-HDE,

suggesting the possible presence of S1P lyase in the nucleus, which could degrade S1P to Δ2-HDE [18, 19]. Here, we report the presence and activity of S1P lyase in the nuclear fractions of lung epithelial cells, and blocking S1P lyase activity with 4-deoxypyridoxine (4-DP), an analog of pyridoxal phosphate, decreased nuclear Δ2-HDE levels in response to *P. aeruginosa* challenge compared to control cells. Further, inhibition of SPHK2 with ABC294640 or downregulation of PKC δ reduced *P. aeruginosa*-induced Δ2-HDE levels in the nucleus. In vitro, exogenous addition of Δ2-HDE inhibited HDAC1/2 activity and increased histone acetylation in nuclear preparations from lung epithelial cells.

Experimental Procedures

Cell Culture

Mouse lung epithelial cells (MLE-12) were cultured in Dulbecco's Modified Eagle Medium (DMEM) complete medium (4.5 g/l glucose), glutamate, sodium pyruvate, non-essential amino acids, heat-inactivated 10% fetal bovine serum (FBS), and 100 U/mL penicillin and streptomycin at 37 °C and 5% CO_2 and were grown to ~90% confluence in 35-mm or 100-mm petri-dishes. Primary human bronchial (Catalog #: CC-2540) and small airway epithelial cells (SAEpCs) (Catalog #: CC-2547), BEBM bronchial epithelial cell basal medium (Catalog #:CC-3171) and growth supplement kit (Catalog #: CC-4175) were purchased from Lonza Bioscience (Basel, Switzerland). Cells were grown in complete BEGM media and used up to passage 8. Murine embryonic fibroblasts (MEFs) were isolated from wild-type (*sgpl1*$^{+/+}$) and *Sgpl1* deficient (*Sgpl1*$^{-/-}$) embryos and provided by Dr. Paul P. Van Veldhoven [20]. MEFs were cultured in DMEM medium (4.5 g/l glucose) with 10% FBS, 100 U/mL penicillin and streptomycin, glutamate, sodium pyruvate, and non-essential amino acids at 37 °C and 5% CO_2.

Animal and Animal Procedures

All animal protocols were approved by the University of Illinois at Chicago Institutional Animal Care Committee (Protocols ACC#12–246 and 18–201). Wild type (*Sgpl1*$^{+/+}$) (129/SV background) derived by breeding *Sgpl1* heterozygous (*Sgpl1*$^{+/-}$) mice (provided by Dr. Philip Soriano, Seattle, WA, USA), and the *Sgpl1*$^{+/-}$ mice were maintained at UIC BRL barrier facility with free access to food and water. Both male and female mice, 8 weeks old were intratracheally administered 20 μl of sterile PBS or live *P. aeruginosa* (1×10^6 CFU/mouse) in 20 μl of sterile PBS as described [14]. Dorsal sub-cutaneous injection of Buprenorphine (0.1 mg/kg) was administered for operative analgesia. After 24 h, the mice were anesthetized with Ketamine (100 mg/kg body weight), Xylazine (5 mg/kg body weight), bronchoalveolar lavage (BAL) fluid was collected using 1 mL of sterile Hanks Balanced Salt buffer. Total infiltrating cells in BAL fluids were performed using a cytospin equipment.

Exposure of Lung Epithelial Cells to Heat-inactivated *P. aeruginosa*

MLE-12 lung epithelial cells grown to ~90% confluence, were starved for 12–18 h in DMEM medium with 2% FBS, without antibiotics, before exposure to heat-inactivated *P. aeruginosa* (1×10^8 CFU/ml) for 3–24 h [15]. Control cells were treated with endotoxin-free sterile saline. Cells were harvested, cell lysates were prepared in 1 × cell lysis buffer (Cell

Lysis Buffer, 10X; Catalog # 9803 Cell Signaling, Beverly, MA, USA) containing protease and phosphatase inhibitors. Total proteins in cell lysates were assayed using BCA protein assay kit (Thermo Fisher Scientific, Waltham, MA, USA).

Overexpression of *SGPL1* in Mouse Lung Epithelial Cells

Infection of MLE-12 cells with purified adenoviral empty or adenoviral vector containing h*SGPL1* cDNA was carried out. Briefly, control or h*SGPL1* wild-type adenoviral constructs (50 MOI) were added to MLE-12 cells (~60% confluence) in DMEM medium containing heat-inactivated 10% FBS. After overnight infection, the medium was replaced with fresh complete medium for another 24 h, before *P. aeruginosa* challenge.

Isolation of Nuclear Fraction from Lung Epithelial Cells

Nuclei from MLE-12 cells or primary human bronchial epithelial cells (HBEpCs) (~90% confluence) were prepared using buffers containing digitonin and NP40 detergents by differential centrifugation. Briefly, nuclei were prepared from MLE-12, human bronchial epithelial, human lung endothelial cells, or lung fibroblasts, grown in 100-mm dishes. Cells were challenged with vehicle or heat-inactivated *P. aeruginosa* (1×10^8 CFU/ml) infection for 2 h, washed three times with PBS, trypsinized with 0.5 ml trypsin, 3 ml of DMEM medium containing 10% FBS was added to neutralize the excess trypsin, cells were detached using a cell scrapper and centrifuged at 1000 × *g* for 10 min at 4 °C. The supernatant was aspirated and cell pellet was resuspended in 1 ml of ice-cold PBS, and centrifuged at 1000 × *g* for 10 min at 4 °C. The pellet was resuspended in 400 μl of ice-cold Buffer A [50 mM HEPES pH 7.4 containing 150 mM NaCl, 25 μg/ml of digitonin, and protease + phosphatase inhibitors], incubated on ice for 10 min followed by centrifugation at 500 × *g* for 5 min. The supernatant was collected (cytosol-enriched fraction) and the pellet was washed in ice-cold PBS and centrifuged at 500 × *g* for 5 min. The supernatant was discarded, and the pellet was resuspended in ice-cold Buffer B [50 mM HEPES pH 7.4 containing 150 mM NaCl and 1% NP40 detergent, and protease + phosphatase inhibitors], and incubated on ice for 30 min with intermittent mixing every 10 min. At the end of 30 min, the microfuge tubes were centrifuged at 7000 × *g* for 5 min at 4 °C and the supernatant was collected and stored as ER and other membrane fraction. The pellet was resuspended in 1 ml ice-cold PBS, and centrifuged at 500 × *g* for 5 min at 4 °C. The nuclear pellet was collected, and resuspended in 25 mM HEPES buffer, pH 7.4. In experiments measuring S1P lyase activity, the nuclear fraction pellet was reconstituted in buffer B (100–400 μl). The purity of the nuclear preparation was determined by transmittance electron microscopy (TEM), western blotting, and immunostaining for lamin B (nuclear marker), ERP72 (ER marker), and lactate dehydrogenase (LDH) [14].

Processing of Specimens for Transmission Electron Microscopy

The nuclear pellets, fixed in 2.5% buffered glutaraldehyde solution (pH 7.2–7.4), were then washed in 0.1 M Sorensen's sodium phosphate buffer (SPB, pH 7.2) and postfixed in buffered 1% osmium tetroxide for 1.5 h. After several buffer washes, samples were dehydrated in an ascending concentration of ethanol leading to 100% absolute ethanol, followed by two changes in propylene oxide (PO) transition fluid. Specimens were infiltrated overnight in a 1:1 mixture of PO and LX-112 epoxy resin, and 2 h in 100%

pure LX-112 resin, and then placed in a 60 °C oven to polymerize (3 days). Semi-thin sections (0.5–1.0 μm) were cut and stained with 1% Toluidine blue-O to confirm the regions of interest (via LM). Ultra-thin sections (70–80 nm) were cut using a Leica Ultracut UCT model ultramicrotome, collected onto 200-mesh copper grids and contrasted with 6% uranyl acetate, and Reynold's lead citrate stains, respectively. Specimen were examined using a JEOL JEM-1220 transmission electron microscope (TEM, operating at 80 kV). Digital micrographs were acquired using a Gatan Erlangshen ES1000W model 785 CCD camera and Digital Micrograph software (Version 1.7).

Immunoblotting

Total cell lysates (20–30 μg protein) were separated on a 10 or 4–20% SDS-PAGE followed by western blotting, as described previously [14, 15]. Proteins were probed by immunoblotting using specific antibodies, HRP-conjugated anti-rabbit or anti-mouse secondary antibody, and detected using enhanced chemiluminescence.

Lipid Extraction and Quantification of Sphingoid Bases and Δ2-HDE by LC-MS/MS

Lipids from cells or subcellular fractions were extracted [21] and phase separated with the use of 2% formic acid as described [22, 23]. Briefly, d7-S1P (30 pmol), d7-16:0-ceramide (*N*-16:0-d7-Sph, 60 pmol) and d7-Sph (30 pmol) and (2E)-hexadecenal-(15,15,16,16-d5) were employed as internal standards and were added during the initial step of lipid extraction. The extracted lipids were dissolved in methanol/chloroform (4:1, v/v), and aliquots were taken to determine total phospholipid content [24]. Samples were concentrated under a stream of nitrogen, re-dissolved in methanol, transferred to auto sampler vials, and subjected to sphingolipid LC-MS/MS analysis. All standards were from Avanti Polar Lipids (Alabaster, AL). Analyses of (2E)-hexadecenal, sphingoid base-1-phosphates, ceramides, and sphingoid bases were performed by electrospray ionization tandem mass spectrometry (ESI-LC/MS/MS). The instrumentation employed was Sciex 6500 QTRAP hybrid triple-quadrupole linear ion-trap mass spectrometer (AB Sciex, Redwood City, CA) equipped with an Ion Drive Turbo V ion spray ionization source interfaced with a Shimadzu Nexera X2 UHPLC system. All lipid molecules and their chemical derivatives were separated using Ascentis Express RP-Amide 2.7 μm 2.1 × 50 mm column and gradient elution from methanol:water:formic acid (65:35:0.5 mM ammonium formate) to methanol:chloroform:water:formic acid (90:10:0.5:0.5 mM ammonium formate). S1P was analyzed as *bis*-acetylated derivatives with d7-S1P as the internal standard employing negative ion ESI and multiple reaction monitoring (MRM) analysis basically as described [22]. (2E)-Hexadecenal was quantified as its semicarbazone derivative that exhibited strong molecular ions at m/z 296.4, m/z 279.4, and m/z 253.4 [23].

S1P Lyase Activity

S1P lyase activity was measured using a synthetic fluorogenic analog of S1P, namely 2-S-ammonio-3R-hydroxy-5 [(2-oxo-2H-chromen-7-yl)oxyl] pentyl hydrogen phosphate (Cayman Chemicals, Item # 13238). The substrate was dissolved in DMSO to a final concentration of 10 mM, aliquoted and stored in −80 °C. The reaction was carried out in 25 mM HEPES buffer pH 7.4 containing 1% NP40 detergent, 50 μM substrate, and 20–50 μg protein, 1 mM pyridoxal phosphate and total cell lysate, ER, or nuclear fraction in a

final volume of 200 µl at RT. The nuclear pellet was sonicated in 25 mM HEPES buffer containing 1% NP40 detergent. The cleavage of the substrate was monitored by measuring the fluorescence of the released product 7-hydroxycoumarin in a spectrofluorimeter. All assays were carried out with the saturating levels of substrate and within the linear range of the activity. The S1P lyase activity was plotted as Relative Fluorescent Unit × (10^3). Appropriate controls with no cell fraction and/or no pyridoxal phosphate and S1P lyase inhibitor (S1PL-IN-31) (2 µM) were included in all the assays.

HDAC1/2 Activity

HDAC1/2 activity in total cell lysates, and nuclear fraction was measured using a commercial kit (Catalog #: 10011563, Cayman Chemicals, Ann Arbor, MI, USA) according to the manufacturer's instructions. This assay is based on the deacetylation of an acetylated lysine substrate by the sample containing HDAC activity. Deacetylation of the acetylated lysine substrate releases a fluorescent product analyzed using a fluorescence plate reader with excitation wavelengths of 340–360 nm and emission wavelengths of 440–465 nm. A deacetylated standard curve (0–84 µM) is included to calculate the deacetylated lysine compound concentration from the linear regression of the standard curve. Deacetylated compound [µM] = [(CSF-Y-intercept)/Slope] where CSF is the corrected sample fluorescence. Trichostatin (TSA), a pan inhibitor of HDAC activity, is included as a control during the analysis. HDAC activity was calculated using the definition: One unit is defined as the amount of enzyme that will liberate 1.0 nmol of the deacetylated compound/min at 37 °C. HDAC Activity (nmol/min/ml) = [µM/30 min] × sample dilution. The dynamic range of the kit was 0–120 nom/min/ml of HDAC activity as provided by the manufacturer. For experiments to determine HDAC1 activity using either the recombinant HDAC1 (rHDAC1 Cat # 31504, Active Motif, Carlsbad, CA, USA; Molecular Weight 56 kDa), or nuclear preparations, the rHDAC1 (50 µg) was reconstituted in assay buffer to obtain a 1 µM final concentration. To the assay buffer (25 mM Tris-HCl, pH 8.0, 137 mM NaCl, 2.7 mM KCl, and 1 mM $MgCl_2$) was added 100 nM of rHDAC1 or nuclear preparation (20–50 µg protein), and the reaction was initiated by the addition of 200 µM HDAC substrate (Cayman Item # 10006392 in the kit) in a final volume of 100 µl. The fluorescence was monitored with the excitation wavelength between 340 and 360 nm and emission wavelength between 440 and 465 nm.

In vitro Adduction of Recombinant HDAC1 by Δ2-hexadecenal

Recombinant human HDAC1 (with His-tag, from Enzo Life Sciences, Lörrach, Germany) was adducted in vitro and the protein adducts formed were detected according to our published method [25]. Briefly, 0.4 mg/ml rHDAC1 (total amount 50 µg) provided in a buffer consisting of 50 mM Tris (pH 8), 138 mM NaCl, and 10% glycerol was incubated with 1 mM Δ2-HDE (Avanti Polar Lipids) at 37 °C for 1 h under gentle shaking (300 rpm). Fatty acid-free human serum albumin (HSA), equally concentrated in the abovementioned HDAC buffer, served as positive control. The protein-free negative control sample contained the buffer alone. To scavenge unreacted Δ2-HDE, the samples were then incubated for another hour at 37 °C with a tenfold molar excess of N-acetyl-L-cysteine (Sigma-Aldrich, Taufkirchen, Germany). Afterwards, samples were rebuffered by means of Amicon Ultra Centrifugal Filter Units (0.5 ml, 3 kDa cut-off) from Merck Millipore (Darmstadt, Germany)

followed by overnight protein hydrolysis at 37 °C (300 rpm) with 50 μg pronase E from *Streptomyces griseus* (Sigma-Aldrich) in a total volume of 800 μl potassium phosphate buffer (50 mM, pH 8.5). Extraction of adducted amino acids was achieved with an equal volume of water-saturated 1-butanol accompanied by extensive shaking for 10 min. The upper organic phase was evaporated to dryness using a Savant SpeedVac concentrator (Thermo Fisher Scientific, Dreieich, Germany). Finally, dried residues were reconstituted in 50 μl methanol and Δ2-HDE-adducted amino acids were analyzed by LC-ESI-MS/MS with a 1260 Infinity HPLC coupled to a 6490 triple-quadrupole mass spectrometer (Agilent Technologies, Waldbronn, Germany) as described previously [25].

ChIP Assay

MLE-12 cells grown to ~90% confluence on 100-mm dishes were treated with heat-killed *P. aeruginosa* (1×10^8 CFU/ml) for 3 h. Formaldehyde was added directly to the cell culture medium to a final concentration of 1% and incubated for 9 min. Glycine was then added to a final concentration of 125 mM and dishes were incubated in room temperature for 5 min, washed with PBS, cells were collected in a 15 ml tube, centrifuged at 800 × *g* for 5 min, and pellet was collected. The pellet was resuspended in chromatin immunoprecipitation (ChIP) lysis buffer (Santa Cruz Biotechnology, Texas, USA) with protease and phosphatase inhibitors, and incubated at 4 °C with rotation for 10 min. Samples were centrifuged at 2000 × *g* for 5 min and 1 ml Micrococcus nuclease digestion buffer containing $CaCl_2$ was added to re-suspend the pellet, and samples were incubated at 37 °C for 10 min. EDTA was added to a final concentration of 5 mM and samples were sonicated three times, 12 s each, at a power of 6. Lysates were centrifuged at 10,000 × *g* for 10 min. Overall, 50 μl of chromatin was removed for analysis and the remaining supernatant was stored at −80 °C. For chromatin analysis, 100 μl of nuclease-free water, 6 μl of 5 M NaCl, and 2 μl RNAse A was added to the 50 μl sample and incubated at 37 °C for 30 min. Following incubation, 2 μl Proteinase K was added and samples were incubated at 65 °C for 2 h. DNA was purified using Qiagen QiA Quick PCR purification kit; protein concentration was measured with a NanoDrop (ThermoFisher, USA) and the amount of digested DNA was viewed by loading 10 μl of sample on a 1.2% agarose gel with 100 bp DNA marker. Overall, 10 μg of digested chromatin was used for each immunoprecipitation (IP). Overall, 50 μl protein A/G agarose beads were added to the digested DNA and samples were incubated for 1 h at 4 °C with rotation. Samples were centrifuged at 4000 × *g* for 5 min and the supernatant was transferred to a new tube. Overall, 10 μl of supernatant was kept aside for input fraction. Chromatin DNA was immunoprecipitated using 5 μg Acetylated Histone H3K9 antibody, 2 μg of negative control (IgG), and 2 μg of positive control ($H_3K_4Me_3$) for 4 h at 4 °C with rotation. Overall, 50 μl of protein A or G magnetic beads were added and samples were incubated for 2 h at 4 °C with rotation. Magnetic beads were pelleted using DynaMag-2 magnet stand (Invitrogen) and supernatant discarded. Magnetic pellets were washed with low salt wash buffer, high salt wash buffer, LiCl wash buffer, and 1 × TE buffer, twice. Overall, 250 μl of Elution buffer was added to input fractions and allowed to incubate at room temperature for 30 min with rotation. Samples were then incubated overnight at 65 °C. Samples were treated with 2 μl RNAse for 30 min at 37 °C. After incubation, 2 μl proteinase K was added and incubated for 1 h at 55 °C. Magnetic beads were pelleted and supernatant was collected; DNA was isolated using Qiagen QIAquick PCR purification kit. Real-time PCR was

performed using specific primers designed to amplify NF-kB binding site in IL-6 proximal promoter region. Primers for IL-6: Forward, 5′-CCAAGAGGTGAGTGCTTCCC-3′, and IL-6 Reverse Primer, 5′-CTGTTGTTCAGACTC TCTCCCT-3′, were obtained from IDT, Coralville, IA.

Statistical Analysis

Data are expressed as mean ± SE from three independent experiments in triplicates unless otherwise indicated. Analysis of variance and Student–Newman–Keuls test was used to compare means of two or more treatment groups. $P < 0.05$ was considered statistically significant. Survival analysis was performed using Kaplan Meier Survival analysis using GraphPad Prism 7. A-log rank test p-value <0.05 was deemed significant. Statistical tests were performed using GraphPad Prism version 7.0, GraphPad Software, La Jolla California, USA.

Results

P. aeruginosa Stimulates Generation of S1P and Δ2-hexadecenal in Nuclei of Lung Epithelial Cells

We have earlier shown that *P. aeruginosa* infection of lung epithelial cells resulted in PKC δ-dependent phosphorylation of SPHK2, its translocation to the nucleus, and generation of S1P in the nucleus [14, 15]. The fate of nuclear S1P is unclear but could be degraded by S1P phosphatases to Sph and/or S1P lyase to ethanolamine phosphate and Δ2-HDE. As S1P lyase is predominantly localized in the ER, we sought to determine if S1P lyase is also present in the nucleus of lung epithelial cells. The nuclear fraction isolated from MLE-12 cells was checked by TEM, and as shown in Fig. 1A, the nuclear fraction exhibited minimal contamination of ER membranes. The purity of the nuclear fraction was also confirmed by immunostaining for cytosol, ER, and nuclear markers. The nuclear preparations from MLE-12 cells revealed no significant contamination of ER membranes (ERP72 and Calnexin markers) and cytosol (LDH marker) (Fig. 1B). Having established the purity of the nuclear preparation, next we determined the levels of sphingoid bases and Δ2-HDE in the nuclear fraction. Stimulation of MLE-12 cells with *P. aeruginosa* did not alter Sph, ceramide or dihydroceramide levels in the nuclear fraction; however, the levels of S1P, Δ2-HDE, and dihydro Sph were elevated compared to PBS controls. (Fig. 1C, D). A similar increase in S1P (~2.5-fold) and Δ2-HDE (~threefold) was seen in nuclei isolated from primary HBEpCs (S1P-control: 4.5 ± 1.2 pmol/mg protein, *P. aeruginosa* treatment for 3 h: 10.2 ± 1.4 pmol/mg protein; Δ2-HDE-control: 5.8 ± 0.6 pmol/mg protein, *P. aeruginosa*-18.6 ± 1.9 pmol/mg protein). Furthermore, pre-treatment of MLE-12 cells with 4-DP that competes for the pyridoxal phosphate binding site on S1P lyase, attenuated *P. aeruginosa*-mediated accumulation of Δ2-HDE in the nuclear, but not the cytoplasm fraction (Fig. 1E). In addition, the S1P levels were elevated both in the cytoplasm and nuclear fractions from 4-DP-treated cells with or without *P. aeruginosa* challenge (Fig. 1E). As *P. aeruginosa*-induced IL-6 secretion in lung epithelium is mediated by PKC δ-dependent SPHK2 activation and its translocation to the nucleus [15], we next determined their role in Δ2-HDE production in the nucleus. Stimulation of MLE-12 cells with *P. aeruginosa* enhanced accumulation of both S1P and Δ2-HDE in the nucleus, which was blocked by a

dominant-negative mutant of PKC δ and ABC294640, an inhibitor of SPHK2, respectively (Fig. 1F, G). These results demonstrate that stimulation of lung epithelial cells with *P. aeruginosa* enhances S1P levels in the cytosol and nuclear fractions, and Δ2-HDE levels only in the nuclear fraction, which was reduced by 4-DP, suggesting catabolism of S1P to Δ2-HDE by S1P lyase in the nucleus.

Immunostaining and Activity of S1P Lyase in Nuclear Fractions of Lung Epithelial Cells and Inhibition of S1P Lyase Reduces *P. aeruginosa*-stimulated Nuclear Δ2-hexadecenal

Having demonstrated enhanced the accumulation of Δ2-HDE in MLE-12 nuclear fractions after stimulation with *P. aeruginosa*, we investigated if S1P lyase could be detected in the nuclear fractions of MLE-12 and other lung cells. Total cell lysates, ER, and nuclear preparations from MLE-12 cells showed immunostaining for S1P lyase (*Sgpl*1 polyclonal antibody; Invitrogen PA1–12722, Lot UF2750922) by western blotting (Fig. 2A). Although we loaded equal protein, the nuclear fraction exhibited stronger immunostaining for S1P lyase compared to the ER fraction. In addition to lung alveolar epithelial cells, HBEpCs, SAEpCs, and human lung microvascular endothelial cells also showed localization of S1P lyase, both in the ER and nuclear fractions (Fig. 2B–D). Next, we determined if S1P lyase expressed in the nucleus is catalytically active by using a synthetic S1P analog as substrate. As shown in Fig. 2E, of the total S1P lyase activity in the cell lysate, ~80% of the activity was recovered in the ER fraction; however, ~20% of the total activity was associated in the nuclear preparations. Pre-treatment of MLE-12 cells with S1P lyase inhibitors, 4-DP, or S1PL-IN-31 (AOBIOUS, Cat # AOB31664) blocked S1P lyase activity in nuclear fractions (Fig. 2F). However, the S1P lyase inhibitor, 2-acetyl-5-tetrahydroxybutyl imidazole that requires transformation to an active metabolite when administered in vivo to mouse, had no effect on the activity in lung alveolar epithelial cells. These results show the localization and activity of S1P lyase in the nuclear fraction, in addition to its predominant distribution in the ER of lung epithelial and other cell types.

S1P Lyase Activity is Essential for *P. aeruginosa*-induced Histone Acetylation in Lung Epithelial Cells

Having established S1P lyase localization and its activity in the nuclear fraction, next we investigated the role of S1P lyase protein or its activity in modulating histone acetylation. Stimulation of MLE-12 cells with *P. aeruginosa* increased H3K9 and H4K8 histone acetylation in the nuclear fraction, which was attenuated by 4-DP (Fig. 3A). Further, the downregulation of $Sgpl1^{+/+}$ with siRNA reduced *PA*-mediated H3K9 and H4K8 histone acetylation (Fig. 3B). Interestingly, ecto-expression of h$SGPL1^{+/+}$ in MLE-12 cells enhanced H3K9 and H4K8 histone acetylation without the addition of *P. aeruginosa* and no additional increase in histone acetylation was observed after challenging the cells with heat-inactivated bacteria (Fig. 3C). The requirement of S1P lyase in *P. aeruginosa*-induced histone acetylation was confirmed in fetal mouse fibroblasts (MEF) isolated from wild-type and *Sgpl1* KO mice. Stimulation of WT $Sgpl1^{+/+}$, but not the $Sgpl1^{-/-}$, MEF cells with *P. aeruginosa* showed increased H4K8 histone acetylation (Fig. 3D). These results show a role for $Sgpl1^{+/+}$ gene product, S1P lyase, in *P.* aeruginosa-induced histone acetylation in lung epithelial cells.

Δ2-Hexadecenal Stimulates Histone Acetylation of Lung Epithelial Nuclear Fraction

Having demonstrated a role for S1P lyase in *P. aeruginosa*-induced histone acetylation in MLE-12 cells, next we investigated if exogenously added Δ2-HDE modulates histone acetylation in the nuclear fraction. Nuclear preparations from MLE-12 cells incubated with Δ2-HDE increased H3K9 and H4K8 histone acetylation in a dose-dependent fashion (0.1–10.0 μM) (Fig. 4A). In contrast to Δ2-HDE, hexadecanal showed less stimulation of histone acetylation at 0.1 and 1 μM levels (Fig. 4A). 2-chlorohexadecanal (0.1–10 μM) exhibited no increase in H3K9 and H4K8 acetylation; however, at a higher dose (50 μM) stimulated H3K9 histone acetylation (Fig. 4B). Interestingly, 4-hydroxynonenal, a short-chain aldehyde derived by lipid peroxidation of polyunsaturated fatty acids, was a potent inducer of H3K9 and H4K8 acetylation in MLE-12 nuclear preparations (Fig. 4C). The stimulatory effect of exogenously added Δ2-HDE on histone acetylation was not dependent on S1P lyase as nuclear preparations from *Sgpl1*$^{+/+}$ and *Sgpl1*$^{-/-}$ MEF cells exhibited similar acetylation profile (Fig. 4D). Furthermore, exogenously added S1P to nuclear fraction of *Sgpl1*$^{+/+}$, but not *Sgpl1*$^{-/-}$, MEF cells modulated histone acetylation at different time periods (Fig. 4D). These results highlight the ability of Δ2-HDE, S1P and to a lesser extent hexadecanal but not chlorohexadecanal, to modulate H3 and H4 histone acetylation in nuclear preparations from lung epithelial cells.

Δ2-Hexadecenal Modulates HDAC Activity in Nuclear Fraction

Histone acetylation is regulated by histone acetyltransferases (HATs) and HDACs [26], and we have previously shown that HDAC activity was inhibited in mouse lungs infected by *P. aeruginosa* [15]. Next, we determined if Δ2-HDE modulated HDAC activity in epithelial cell nuclear fraction and rHDAC1. The HDAC1 activity, as measured by deacetylation of a synthetic lysine acetylated peptide, was dependent on the nuclear protein concentration (Fig. 5A). Next, the nuclear fractions from MLE-12 cells were incubated with varying concentrations of Δ2-HDE, S1P or TSA as a control HDAC inhibitor, and the activity (fluorescence) was monitored with an excitation wavelength of 340–360 nm and emission wavelength of 440–465 nm. Addition of Δ2-HDE, in a dose-dependent manner (0.01–1.0 μM), inhibited HDAC1 activity in the nuclear fraction (Fig. 5B). Similarly, S1P (0.01–1 μM) also exhibited inhibition of nuclear HDAC1 activity (Fig. 5C), which could be explained by the hydrolysis of S1P to Δ2-HDE by nuclear S1P lyase activity. TSA, a nonspecific inhibitor of HDAC, blocked (>80%) of the nuclear HDAC activity (Fig. 5B). A similar inhibition of rHDAC1 activity by Δ2-HDE, but not S1P, was observed (Fig. 5D). The inability of S1P to block rHDAC1 activity could be explained by the lack of S1P lyase activity in rHDAC1. While lower concentrations of Δ2-HDE inhibited HDAC1/2 activity in nuclear preparations from MLE-12 cells and rHDAC1, higher concentrations of Δ2-HDE (>5 μM) activated HDAC1/2 activity (Fig. 5E). Nuclear fractions isolated from MLE-12 cells, pretreated with 4-DP (an inhibitor of S1P lyase), exhibited lower HDAC1 activity compared to cells not treated with 4-DP (Fig. 5F). Next, we determined HDAC activity in nuclear fractions from *Sgpl1*$^{+/+}$ WT and *Sgpl1*$^{-/-}$ MEF cells. The HDAC activity in nuclear fractions from *Sgpl1*$^{+/+}$ and *Sgpl1*$^{-/-}$ MEF cells under basal conditions were similar; however, inhibition of HDAC activity in nuclear fractions from *P. aeruginosa* treatment was more pronounced in *Sgpl1*$^{+/+}$ MEF cells compared to *Sgpl1*$^{-/-}$ MEF cell*s* (Fig. 5G).

Δ2-Hexadecenal Forms Adducts with HDAC1 in vitro

To investigate a possible mechanism of HDAC1/2 inhibition by Δ2-HDE, recombinant human HDAC1 was incubated with Δ2-HDE in vitro and subsequently protein adducts of the α, β-unsaturated aldehyde were analyzed by LC-MS/MS. HSA was included as a positive control, since we could already show adduct formation by Δ2-HDE with this model protein [25]. We were able to detect a total of five different amino acid adducts in extracted protein hydrolysates of rHDAC1. By far the most abundant adduct was the Schiff base (imine) product of Δ2-HDE with lysine (Δ2-HDE-Lys), followed by Michael adducts with cysteine (3-Cys-HDE), histidine (3-His-HDE), tryptophan (3-Trp-HDE), and arginine (3-Arg-HDE) (Fig. 6A–E). The identity of these adducts was proven by measuring four mass transitions each in the MRM mode. Histidine adducts may also have been formed at least partially with the His-tag of rHDAC1. The exceptionally high lysine adduct levels—based on peak areas they were about 50 times higher than those of the cysteine adducts placed second-might be explained by the relatively high number of lysine residues (40 out of 482 aa) in the primary structure of HDAC1. However, the mere number is probably less decisive than the exposed position on the protein's surface and thus accessibility for the electrophile. This is because HSA, which was adducted, processed, and analyzed in an analog manner, showed less than 10% of Δ2-HDE-Lys levels found in rHDAC1 (Fig. 6F) with a comparable number of Lys residues in its sequence (60 out of 609 aa). Our in vitro experiments thus show that Δ2-HDE readily reacts with HDAC1 and generates Lys adducts, which are over-represented on the protein's surface. It is therefore conceivable that an increase in nuclear Δ2-HDE could lead to a modification and associated functional impairment of HDAC1/2.

Genetic Deletion of *Sgpl1* Attenuates *P. aeruginosa*-induced Inflammation in Mouse Lung

We have earlier shown that the inhibition of S1P lyase in mice confers protection against LPS-induced lung injury [27] and genetic deletion of *Sgpl1* (S*gpl1*$^{+/-}$) in mice reduced mechanical ventilation mediated lung injury [28]. To assess the role of S1P lyase in *P. aeruginosa*-mediated lung injury, wild-type (129/SV) and *Sgpl1*$^{+/-}$ (129/SV) mice were challenged with vehicle or *P. aeruginosa* (1×10^6 CFU/mouse) for 24 h, as described previously [15, 28]. Deletion of both alleles of *Sgpl1* gene in mice results in defective vascular development and lethality between 4 and 8 weeks after birth [28]. We have shown earlier that *Sgpl1* mRNA and protein expression of S1P lyase were reduced ~50% in *Sgpl1*$^{+/-}$ mice compared to the wild type [28]. Evaluation of BAL fluid from wild type revealed significant increase in total cell counts exposed to *P. aeruginosa*, and deletion of one allele of *Sgpl1* gene (*Sgpl1*$^{+/-}$) in mice decreased the infiltration of inflammatory cells into the alveolar space (Fig. 7A). To further examine whether *P. aeruginosa* modulates histone acetylation pattern at IL-6 promoter, ChIP assays were performed using anti-acetyl histone H3K9 antibody. *P. aeruginosa A* increased H3K9 histone acetylation at nuclear factor kappa B (NF-κB) binding sites on IL-6 promoter at 3 h post infection, which was blocked by S1P lyase inhibitor 4-DP (Fig. 7B). Collectively, these results show for the first time a role for S1P lyase activity in *P. aeruginosa*-mediated regulation of chromatin modification in IL-6 promoter regions of NF-κB binding site(s) in lung epithelial cells.

Discussion

The present study demonstrates, for the first time, nuclear localization of S1P lyase and its role in the generation of Δ2-HDE in the nucleus of lung epithelial cells, in response to *P. aeruginosa* challenge. Also, Δ2-HDE generated in the nucleus regulated HDAC1/2 activity, and H3 and H4 histone acetylation. Further, in vitro, Δ2-HDE formed Schiff base (imine) products with lysine (Δ2-HDE-Lys), accompanied by Michael adducts with cysteine (3-Cys-HDE), histidine (3-His-HDE), tryptophan (3-Trp-HDE), and arginine (3-Arg-HDE). Our results strongly suggest a role for nuclear S1P lyase-mediated and Δ2-HDE-dependent modulation of chromatin remodeling in lung epithelial cells exposed to bacterial infection. In the nucleus, the levels of S1P, the substrate for S1P lyase, are much lower compared to the total cellular or plasma levels [6]; however, *P. aeruginosa* infection of lung epithelial cells enhanced the nuclear S1P and Δ2-HDE levels compared to controls. Blocking S1P lyase activity or the downregulation of *Sgpl1* reduced nuclear Δ2-HDE levels and histone acetylation pattern in lung epithelial cells, in contrast to cell lysates. S1P lyase is a pyridoxal phosphate-dependent enzyme that cleaves the acyl chain between carbon atom 2 and 3 of S1P or dihydro S1P to Δ2-HDE or hexadecanal, respectively, in mammalian cells [11]. It is predominantly localized in the ER inner membrane with the catalytic site facing the cytosol [12]. Here we show the localization of S1P lyase in the nuclear fraction that is mostly devoid of ER membranes and cytosol. The immunoblots with various subcellular fraction markers (Fig. 2) indicate that the nuclear preparation has very minimal (<5%) contamination of ER membranes and cytosol. However, the possibility of the nuclear fraction to retain a small fraction of ER membranes attached to it that is not detectable by immunostaining cannot be ruled out due to the limitation of the technique. In addition to immunostaining, we could measure S1P lyase activity in the nuclear fraction, which was ~20% of the measured activity of the crude ER fraction. As the ER fraction had NP40 detergent as per the isolation protocol, the same amount of NP40 was added to the nuclear fraction to maintain same detergent concentration, which could interfere with the activity of S1P lyase [12]. The nuclear localization of S1P lyase was not restricted to lung epithelial cells but was observed in other lung cell types, such as endothelial cells. In addition, partial genetic deletion of *Sgpl1* (*Sgpl1*$^{+/-}$) in mice significantly reduced *P. aeruginosa*-mediated infiltration of pro-inflammatory cells into the alveolar space, compared to wild-type animals, demonstrating a protective role for S1P lyase in bacterial lung inflammatory injury. *P. aeruginosa* infection of mouse lung enhanced the infiltration of neutrophils into the alveolar space, that was blocked by deletion of *Sphk2* or inhibition of SPHK2 activity by administration of ABC294640 in mice (14). Interestingly, in other lung pathologies, inhibition, or genetic deletion of S1P lyase has been shown to protect against mechanical ventilation [28], and sepsis-induced lung injury [27, 29]. On the contrary, S1P lyase is an endogenous suppressor of pulmonary fibrosis in the mouse-bleomycin model wherein partial deletion of *Sgpl1* in mice (*sgpl1*$^{+/-}$) exacerbated bleomycin-induced lung inflammatory injury and pulmonary fibrosis [30]. Thus, the role of S1P lyase may depend on the pathological context and the type of cells involved.

S1P is predominantly generated in the cytoplasmic compartment of cells by SPHK1, while SPHK2 has been shown to generate S1P both in the cytoplasm and nucleus [4, 5]. In

cancer cells, phorbol ester induced nuclear S1P generation via SPHK2 [15], and we have recently shown a critical role for PKC δ-mediated activation of SPHK2 and generation of nuclear S1P in *P. aeruginosa*-mediated acetylation of H3 and H4 histone [14]. While extracellular S1P signals by binding to $S1P_{1–5}$ receptors on the plasma membrane of cells, the nuclear S1P was shown to bind to HDAC and inhibit its activity [15]. Although S1P binds to rHDAC2 or HDAC1/2 in lung epithelial cells [14], its binding to rHDAC2 had no effect on HDAC2 activity (Fig. 5D); however, exogenous S1P inhibited HDAC activity of the nuclear fraction from MLE-12 cells (Fig. 5C). On the contrary, addition of Δ2-HDE to either rHDAC2 or nuclear preparations blocked HDAC activity. The ability of S1P to inhibit HDAC activity in the nuclear fraction and not with the rHDAC1 indicates the role of S1P lyase activity present in the nuclear fraction to cleave S1P to Δ2-HDE that blocked the activity. This is confirmed by experiments carried out with MEF cells isolated from $Sgpl1^{+/+}$ and $Sgpl1^{-/-}$ mice (Fig. 4D). Interestingly, higher concentration of Δ2-HDE, in contrast to lower concentrations, increased HDAC2 activity suggesting a concentration-dependent modulatory effect of Δ2-HDE. In addition, pre-treatment of lung epithelial cells with phloretin, a nonspecific fatty acid uptake inhibitor, and chelator of fatty aldehydes [31], reduced HDAC activity mediated by Δ2-HDE released in the nucleus [13].

Our results suggest modulation of HDAC1/2 activity leading to chromatin remodeling by Δ2-HDE released from S1P by S1P lyase in the lung epithelium; however, the mechanism(s) of this modulation is unclear. Δ2-HDE, has a α, β-unsaturated carbonyl function with two electrophilic centers at C-1 and C-3 carbon atoms, which are susceptible to nucleophilic substitutions. The C-3 carbon atom is a soft electrophile acceptor that forms Michael adducts with nucleophiles, such as thiols; however, the C-1 carbon is a much stronger electrophile that can react with primary amino groups of proteins to generate Schiff bases [19, 32, 33]. We tested the possibility of potential adduct formation between Δ2-HDE and HDAC1 by incubating Δ2-HDE with rHDAC1 in vitro, which yielded five different hexadecenal adducts as determined by LC-MS/MS. The Schiff base between Lys and Δ2-HDE was the most predominant Michael adduct, while adducts of cysteine, histidine, arginine, and tryptophan were also detected at lower levels (Fig. 6). In addition to the formation of adducts with HDAC1, Δ2-HDE formed two conjugates with GSH and seven adducts with L-histidine of BSA and proteins from HepG2 cell lysates [25] demonstrating the ability of Δ2-HDE to form different types of adducts with macromolecules.

In addition to Δ2-HDE, mammalian cells also generate long-chain fatty aldehydes, such as hexadecanal from plasmalogens and lysoplasmalogen by the enzymatic action of plasmalogenase or lysoplasmalogenase, respectively [19, 34, 35], and long-chain halo fatty aldehydes, such as α-chloro or α-bromo fatty aldehydes from plasmalogens by hypochlorous or hypobromous acid released from neutrophil myeloperoxidase [36–38]. Compared to Δ2-HDE, hexadecanal and chlorohexadecanal at lower concentrations were less effective in modulating H3 and H4 histone acetylation, indicating differences in the reactivity of various long-chain aldehydes in chromatin modification. In addition to forming adducts with proteins, Δ2-HDE also reacts with deoxyguanosine and DNA, in vitro, to form diastereomeric cyclic 1,N^2-deoxyguanosine adducts 3-(2-deoxy-β-Derythro-pentafuranosyl)-5,6,7,8-tetrahydro-8R-hydroxy-6R-tridecylpyrimido [1,2-α]purine-10 (3H)one, and 3-(2-deoxy-β-D-erythro-

pentafuranosyl)-5,6,7,8-tetrahydro-8S-hydroxy-6S-tridecylpyrimido[1,2–]purine-10(3H) one [39]. The formation of adducts between Δ2-HDE and HDAC1/2, and other proteins and DNA in the nucleus of lung epithelial cells, after *P. aeruginosa* infection needs to be established. In addition to forming adducts with macromolecules, these long-chain fatty aldehydes are converted to the corresponding fatty acids by fatty aldehyde dehydrogenases, which are recycled back into phospholipids by fatty acyl CoA: acyltransferase or metabolized by beta-oxidation [40].

Studies on signaling and cellular functions of Δ2-HDE and long-chain fatty aldehydes are limited [27, 40–43] despite the importance of S1P lyase in regulating S1P levels in mammalian cells [13, 29]. While it is difficult to determine a direct role of Δ2-HDE released from S1P by S1P lyase in cellular functions under normal and pathological conditions, inhibition or knockdown of S1P lyase has been shown to attenuate LPS- and ventilator-induced lung inflammatory injury [27, 29, 43], and improve cerebral microvascular barrier function after LPS or TNF-α inflammatory challenge [44]. In contrast to the sepsis and ventilator models of lung injury, partial deletion of *Sgpl1* (*Sgpl1*$^{+/-}$) accentuated bleomycin-induced pulmonary fibrosis in mice, suggesting S1P lyase as an endogenous suppressor of pulmonary fibrosis [30]. In the current study, the Δ2-HDE generated by the nuclear S1P lyase modulates HDAC1/2 activity and histone acetylation; however, the role of Δ2-HDE generated in the endoplasmic membrane where most of the S1P lyase is localized is unclear. Interestingly, a recent study showed that SPHK2 generated S1P in the ER suppressed stimulation of interferon genes (STING) signaling in CD11b+ macrophages and thereby facilitating the resolution of lung vascular inflammatory injury [45], wherein S1P generated by SPHK2 interacted with STING and modulate it's signaling. However, it is possible that S1P generated in CD11b+ macrophages was acted by S1P lyase in the ER to generate Δ2-HDE, which could have modulatory effect on STING activity and signaling.

In addition to the intracellular role of Δ2-HDE, there have been a couple of studies demonstrating the ability of exogenously added Δ2-HDE to mediate signal transduction in mammalian cells, although long-chain fatty aldehydes are not easily cell permeable. Exogenous addition of Δ2-HDE to HEK293T, NIH3T3 or HeLa cells induced cytoskeletal reorganization of stress fibers and apoptotic cell death that was mediated by ROS-dependent MLK3/JNK activation, and not dependent on ERK, AKT, and p38 MAPK signaling [28]. In contrast to Δ2-HDE, hexadecanoic acid did not modulate cellular ROS, JNK activation, and apoptosis. Similarly, treatment of glioma C6 cells with Δ2-HDE reduced proliferation and mitotic indices while higher Δ2-HDE (350 μM) induced necrosis and reduced survival [41]. In addition, Δ2-HDE activated ER K1/2, p38 MAPK and JNK, but not PI3K pathways in C6 glioma cells [41]. In these studies, use of high concentrations of Δ2-HDE induced the cytoskeletal changes, and apoptosis. In lung epithelial cells, exogenous Δ2-HDE addition did not activate MAPK or PI3K signaling pathways (data not shown); however, addition of hexadecanal or ethanolamine phosphate stimulated p38 MAPK and Iκ-B phosphorylation [27]. The myeloperoxidase mediated generation of chloro- and bromo-fatty aldehydes from plasmalogens induced loss of endothelial barrier function, apoptosis, mitochondrial dysfunction and altered intracellular redox balance, which were restored by phloretin [46]. It is likely that signal transduction pathways modulated by high concentrations of Δ2-HDE, hexadecanal or halogenated fatty aldehydes were not mediated by specific fatty aldehyde

receptors on the cell surface as to date no such receptors have been cloned. Most likely, the highly reactive long-chain fatty aldehydes interact with and modify cell surface proteins, and receptors, which induce signal transduction to intracellular compartments. In contrast to long-chain aldehydes, short chain aldehyde(s), such as 4-HNE stimulates cellular signaling and function [47, 48]. 4-HNE stimulates many cellular signal transduction pathways by modulating protein kinases [49, 50], receptor tyrosine kinases [51], phospholipase D [52, 53], and endothelial barrier function through focal adhesion kinase and cytoskeletal reorganization [54]. Like Δ2-HDE, 4-HNE also formed deoxyguanosine adducts with DNA [55] and histone residues of chromatin at acetylation and methylation sites of H3K23 and H3K27 in macrophages [56]. Further in vivo and in vitro studies are necessary to understand the physiological and pathophysiological relevance of spatio-temporally generated Δ2-HDE by S1P lyase in the nuclear and cytoplasmic compartments of the cell in modulating cellular functions including chromatin remodeling.

There is evidence for nuclear S1P generation and its role in the modulation of nuclear signaling and chromatin remodeling. The SPHK2 mediated nuclear S1P generation modulates HDAC1/2 activity at least by three different mechanisms. In the first mechanism, binding of S1P or FTY720 to HDAC1/2 inhibits activity and thereby enhancing histone acetylation pattern [15, 16]. In the second mechanism, the *P. aeruginosa*-mediated SPHK2 activation and S1P generation in the nucleus stimulates nuclear reactive oxygen species production via NOX4 with the subsequent oxidation of HDAC1/2 and chromatin remodeling in the lung epithelium [57]. In the current study, generation of nuclear Δ2-HDE from S1P by nuclear S1P lyase modulates HDAC1/2 activity and chromatin remodeling most likely via formation of adducts. Further investigations are necessary to dissect these different mechanisms on nuclear signaling, HDAC1/2 oxidation and modulation of HDAC1/2 activity that is essential for chromatin remodeling and expression of pro-inflammatory genes.

Limitation of Study

We acknowledge that this study has some limitations. The nuclear preparations were mostly free of ER membranes and small contamination with ER membranes cannot be completely excluded. However, our data suggest a small fraction of S1P lyase to be localized in the nucleus that exhibited activity. We focused primarily on the lung epithelial cells in cell culture system to quantify Δ2-HDE generated in the nucleus. Also, we realize that our in vitro formation of adducts between Δ2-HDE and HDAC1/2 must be demonstrated in vivo in the lung epithelium or other cell types after *P. aeruginosa* infection of the mouse lung. In addition to forming adducts with HDACs, Δ2-HDE may interact with other nuclear proteins that are yet to be identified. Quantification of these adducts formed in the nucleus under normal and pathological conditions may provide several technical challenges including immunoprecipitation and mass spectrometry detection and quantification of the adducts. Further, we have investigated the effect of Δ2-HDE on HDAC1/2 activity while its effect on HATs is not known. As histone acetylation is regulated by HDACs and HATs, additional studies are required to address how HATs are modulated by S1P lase generated Δ2-HDE.

Conclusions

Collectively, our findings demonstrate a novel role for nuclear Δ2-HDE generated by SPHK2/S1P pathway by nuclear S1P lyase in the modulation of HDAC1/2 activity and chromatin remodeling in lung epithelium. Our results also show ex vivo the ability of Δ2-HDE to form adducts with rHDAC1 suggesting a pro-inflammatory role of Δ2-HDE in *P. aeruginosa*-mediated lung injury (Fig. 8). Hence, targeting S1P lyase activity or *Sgpl1* in the lung epithelium might be a potentially useful therapeutic strategy against bacterial and other models of lung inflammatory injury.

Acknowledgements

The *P. aeruginosa* 103 strain stock culture was provided by Dr. Ruxana T. Sadikot during her tenure at University of Illinois, Chicago. This work made use of the instrumentation provided by the Electron Microscopy Core of the University of Illinois at Chicago's Research Resources Center. We thank Ms. Figen A. Seiler, M.S. for her excellent services at the UIC Electron Microscopy Core for processing the Transmission Electron Micrographs.

Funding

This work was supported by National Institutes of Health grants HLBI P01HL126609, P01HL060678, R01HL127342 (to VN), and R01 AG069865 (to S.J.K.). The content is solely the responsibility of the authors and does not necessarily represent the official views of the National Institutes of Health.

Data Availability

All data presented and discussed are contained within the manuscript. All the data and materials are available from V.N.

References

1. Kohama T, Olivera A, Edsall L, Nagiec MM, Dickson R, & Spiegel S (1998). Molecular cloning and functional characterization of murine sphingosine kinase. Journal of Biological Chemistry, 273, 23722–23728. [PubMed: 9726979]
2. Liu H, Sugiura M, Nava VE, Edsall LC, Kono K, Poulton S, Milstein S, Kohama T, & Spiegel S (2000). Molecular cloning and functional characterization of a novel mammalian sphingosine kinase type 2 isoform. Journal of Biological Chemistry, 275, 19513–19520. [PubMed: 10751414]
3. Cannavo A, Liccardo D, Komici K, Corbi G, de Lucia C, Femminella GD, Elia A, Beneivenga L, Ferrara N, Koch WJ, Paolocci N, & Rengo G (2017). Sphingosine kinases and sphingosine 1-phosphate receptors: signaling and actions in the cardiovascular system. Frontiers in pharmacology, 8, 556. [PubMed: 28878674]
4. Siow DL, Anderson CD, Berdyshev EV, Skobeleva A, Natarajan V, Pitson SM, & Wattenberg BW (2011). Sphingosine kinase localization in the control of sphingolipid metabolism. Advances in Enzyme Regulation, 51, 229–244. [PubMed: 21075134]
5. Hatoum D, Haddadi N, Lin Y, Nassif NT, & McGowan EM (2017). Mammalian sphingosine kinase (SphK) isoenzymes and isoform expression: challenges for SphK as an oncotarget. Oncotarget, 8, 36898. [PubMed: 28415564]
6. Daum G, Winkler M, Moritz E, Müller T, Geffken M, von Lucadou M, Haddad M, Peine S, Böger R, Larena-Avellaneda A, Debus ES, Gräler M, & Schwedhelm E (2020). Determinants of serum-and plasma sphingosine-1-phosphate concentrations in a healthy study group. TH Open: Companion Journal to Thrombosis and Haemostasis, 4, e12–e19. [PubMed: 31984305]
7. Chung MY, Park SY, Chung JO, Cho DH, & Chung DJ (2020). Plasma sphingosine 1-phosphate concentrations and cardiovascular autonomic neuropathy in individuals with type 2 diabetes. Scientific reports, 10, 1–8. [PubMed: 31913322]

8. Mandala SM (2001). Sphingosine-1-phosphate phosphatases. Prostaglandins & Other Lipid Mediators, 64, 143–156. [PubMed: 11324704]

9. Zhao Y, Kalari SK, Usatyuk PV, Gorshkova I, He D, Watkins T, Brindley DN, Sun C, Bittman R, Garcia JGN, Berdyshev EV, & Natarajan V (2007). Intracellular generation of sphingosine 1-phosphate in human lung endothelial cells: role of lipid phosphate phosphatase-1 and sphingosine kinase 1. Journal of Biological Chemistry, 282, 14165–14177. [PubMed: 17379599]

10. Tang X, Benesch MG, & Brindley DN (2015). Lipid phosphate phosphatases and their roles in mammalian physiology and pathology. Journal of Lipid Research, 56, 2048–2060. [PubMed: 25814022]

11. Aguilar A, & Saba JD (2012). Truth and consequences of sphingosine-1-phosphate lyase. Advances in Biological Regulation, 52, 17–30. [PubMed: 21946005]

12. Van Veldhoven PP, & Mannaerts GP (1991). Subcellular localization and membrane topology of sphingosine-1-phosphate lyase in rat liver. Journal of Biological Chemistry, 266, 12502–12507. [PubMed: 2061324]

13. Ebenezer DL, Fu P, Suryadevara V, Zhao Y, & Natarajan V (2017). Epigenetic regulation of pro-inflammatory cytokine secretion by sphingosine 1-phosphate (S1P) in acute lung injury: role of S1P lyase. Advances in Biological Regulation, 63, 156–166. [PubMed: 27720306]

14. Ebenezer DL, Berdyshev EV, Bronova IA, Liu Y, Tiruppathi C, Komarova Y, Benevolenskaya EV, Suryadevara V, Ha AW, Harijith A, Tuder RM, Natarajan V, & Fu P (2019). Pseudomonas aeruginosa stimulates nuclear sphingosine-1-phosphate generation and epigenetic regulation of lung inflammatory injury. Thorax, 74, 579–591. [PubMed: 30723184]

15. Hait NC, Allegood J, Maceyka M, Strub GM, Harikumar KB, Singh SK, Luo C, Marmorstein R, Kordula T, Milstein S, & Spiegel S (2009). Regulation of histone acetylation in the nucleus by sphingosine-1-phosphate. Science, 325, 1254–1257. [PubMed: 19729656]

16. Gardner NM, Riley RT, Showker JL, Voss KA, Sachs AJ, Maddox JR, & Gelineau- van Waes JB (2016). Elevated nuclear and cytoplasmic FTY720-phosphate in mouse embryonic fibroblasts suggests the potential for multiple mechanism in FTY-720 induced neural tube defects. Toxicol Sci, 150, 161–168. [PubMed: 26719367]

17. Igarashi N, Okada T, Hayashi S, Fujita T, Jahangeer S, & Nakamura SI (2003). Sphingosine kinase 2 is a nuclear protein and inhibits DNA synthesis. Journal of Biological Chemistry, 278, 46832–46839. [PubMed: 12954646]

18. Fu P, Ebenezer DL, Ha AW, Suryadevara V, Harijith A, & Natarajan V (2018). Nuclear lipid mediators: Role of nuclear sphingolipids and sphingosine-1-phosphate signaling in epigenetic regulation of inflammation and gene expression. Journal of Cellular Biochemistry, 119, 6337–6353. [PubMed: 29377310]

19. Ebenezer DL, Fu P, Ramchandran R, Ha AW, Putherickal V, Sudhadevi T, Harijith A, Schumacher F, Kleuser B, & Natarajan V (2020). S1P and plasmalogen derived fatty aldehydes in cellular signaling and functions. Biochimica et Biophysica Acta (BBA)-Molecular and Cell Biology of Lipids, 1865, 158681. [PubMed: 32171908]

20. Colie S, Van Veldhoven PP, Kedjouar B, Bedia C, Albinet V, Sorli S-C, Garcia V, Djavaheri-Mergny M, Bauvy C, Codogno P, Levade T, & Andrieu-Abadie ND (2009). Disruption of sphingosine 1-phosphate lyase confers resistance to chemotherapy and promotes oncogenesis through Bcl-2/Bcl-xL upregulation. Cancer Res, 69, 9346–9353. [PubMed: 19934311]

21. Bligh EG, & Dyer WJ (1959). A rapid method of total lipid extraction and purification. Canadian Journal of Biochemistry and Physiology, 37, 911–917. [PubMed: 13671378]

22. Berdyshev EV, Gorshkova IA, Garcia JG, Natarajan V, & Hubbard WC (2005). Quantitative analysis of sphingoid base-1-phosphates as bisacetylated derivatives by liquid chromatography–tandem mass spectrometry. Analytical Biochemistry, 339, 129–136. [PubMed: 15766719]

23. Berdyshev EV, Goya J, Gorshkova I, Prestwich GD, Byun HS, Bittman R, & Natarajan V (2011). Characterization of sphingosine-1-phosphate lyase activity by ESI-LC/MS/MS quantitation of (2E)-hexadecenal. Analytical Biochemistry, 408, 12–18. [PubMed: 20804717]

24. Vaskovsky VE, Kostetsky EY, & Vasendin IM (1975). A universal reagent for phospholipid analysis. Journal of Chromatography A, 114, 129–141.

25. Schumacher F, Neuber C, Finke H, Nieschalke K, Baesler J, Gulbins E, & Kleuser B (2017). The sphingosine 1-phosphate breakdown product, (2E)-hexadecenal, forms protein adducts and glutathione conjugates in vitro. Journal of Lipid Research, 58, 1648–1660. [PubMed: 28588048]
26. Yang XJ, & Seto EHAT (2007). HATs and HDACs: from structure, function and regulation to novel strategies for therapy and prevention. Oncogene, 26, 5310–5310. [PubMed: 17694074]
27. Zhao Y, Gorshkova IA, Berdyshev E, He D, Fu P, Ma W, Su Y, Usatyuk PV, Pendyala S, Oskouian B, Saba JD, & Natarajan V (2011). Protection of LPS-induced murine acute lung injury by sphingosine-1-phosphate lyase suppression. American Journal of Respiratory Cell and Molecular Biology, 45, 426–435. [PubMed: 21148740]
28. Suryadevara V, Fu P, Ebenezer DL, Berdyshev E, Bronova IA, Huang LS, Harijith A, & Natarajan V (2018). Sphingolipids in ventilator induced lung injury: role of sphingosine-1-phosphate lyase. International Journal of Molecular Sciences, 19, 114.
29. Weigel C, Hüttner SS, Ludwig K, Krieg N, Hofmann S, Schröder NH, Robbe L, Kluge S, Nierhaus A, Winkler MS, Rubio I, von Maltzahn J, Spiegel S, & Gräler MH (2020). S1P lyase inhibition protects against sepsis by promoting disease tolerance via the S1P/S1PR3 axis. EBioMedicine, 58, 102898. [PubMed: 32711251]
30. Huang LS, Berdyshev EV, Tran JT, Xie L, Chen J, Ebenezer DL, Mathew B, Gorshkova I, Zhang W, Reddy SP, Harijith A, Wang G, Feghali-Bostwick C, Noth I, Ma S-F, Zhou T, Ma W, Garcia JGN, & Natarajan V (2015). Sphingosine-1-phosphate lyase is an endogenous suppressor of pulmonary fibrosis: role of S1P signalling and autophagy. Thorax, 70, 1138–1148. [PubMed: 26286721]
31. Mitchell RW, Edmundson CL, Miller DW, & Hatch GM (2009). On the mechanism of oleate transport across human brain microvessel endothelial cells. Journal of Neurochemistry, 110, 1049–1057. [PubMed: 19493158]
32. LoPachin RM, Gavin T, Petersen DR, & Barber DS (2009). Molecular mechanisms of 4-hydroxy-2-nonenal and acrolein toxicity: nucleophilic targets and adduct formation. Chemical Research in Toxicology, 22, 1499–1508. [PubMed: 19610654]
33. Pearson RG (1990). Hard and soft acids and bases—the evolution of a chemical concept. Coordination Chemistry Reviews, 100, 403–425.
34. Jenkins CM, Yang K, Liu G, Moon SH, Dilthey BG, & Gross RW (2018). Cytochrome c is an oxidative stress–activated plasmalogenase that cleaves plasmenylcholine and plasmenylethanolamine at the sn-1 vinyl ether linkage. Journal of Biological Chemistry, 293, 8693–8709. [PubMed: 29530984]
35. Wu LC, Lin YY, Yang SY, Weng YT, & Tsai YT (2011). Antimelanogenic effect of c-phycocyanin through modulation of tyrosinase expression by upregulation of ERK and downregulation of p38 MAPK signaling pathways. Journal of Biomedical Science, 18, 1–11. [PubMed: 21208456]
36. Stadelmann-Ingrand S, Favreliere S, Fauconneau B, Mauco G, & Tallineau C (2001). Plasmalogen degradation by oxidative stress: production and disappearance of specific fatty aldehydes and fatty α-hydroxyaldehydes. Free Radical Biology and Medicine, 31, 1263–1271. [PubMed: 11705705]
37. Albert CJ, Crowley JR, Hsu FF, Thukkani AK, & Ford DA (2001). Reactive chlorinating species produced by myeloperoxidase target the vinyl ether bond of plasmalogens: identification of 2-chlorohexadecanal. Journal of Biological Chemistry, 276, 23733–23741. [PubMed: 11301330]
38. Albert CJ, Crowley JR, Hsu FF, Thukkani AK, & Ford DA (2002). Reactive brominating species produced by myeloperoxidase target the vinyl ether bond of plasmalogens: disparate utilization of sodium halides in the production of α-halo fatty aldehydes. Journal of Biological Chemistry, 277, 4694–4703. [PubMed: 11836259]
39. Upadhyaya P, Kumar A, Byun HS, Bittman R, Saba JD, & Hecht SS (2012). The sphingolipid degradation product trans-2-hexadecenal forms adducts with DNA. Biochemical and Biophysical Research Communications, 424, 18–21. [PubMed: 22727907]
40. Nakahara K, Ohkuni A, Kitamura T, Abe K, Naganuma T, Ohno Y, Zoeller RA, & Kihara A (2012). The Sjögren-Larsson syndrome gene encodes a hexadecenal dehydrogenase of the sphingosine 1-phosphate degradation pathway. Molecular Cell, 46, 461–471. [PubMed: 22633490]

41. Kumar A, Byun HS, Bittman R, & Saba JD (2011). The sphingolipid degradation product trans-2-hexadecenal induces cytoskeletal reorganization and apoptosis in a JNK-dependent manner. Cellular Signalling, 23, 1144–1152. [PubMed: 21385609]
42. Amaegberi NV, Semenkova GN, Kvacheva ZB, Lisovskaya AG, Pinchuk SV, & Shadyro OI (2019). 2-Hexadecenal inhibits growth of C6 glioma cells. Cell Biochemistry and Function, 37, 281–289. [PubMed: 31038222]
43. Saba JD (2019). Fifty years of lyase and a moment of truth: sphingosine phosphate lyase from discovery to disease. Journal of Lipid Research, 60, 456–463. [PubMed: 30635364]
44. Stepanovska B, Lange AI, Schwalm S, Pfeilschifter J, Coldewey SM, & Huwiler A (2020). Downregulation of S1P Lyase Improves Barrier function in human cerebral microvascular endothelial cells following an inflammatory challenge. International Journal of Molecular Sciences, 21, 1240.
45. Joshi JC, Joshi B, Rochford I, Rayees S, Akhter MZ, Baweja S, Chave KR, Tauseef M, Abdelkarim H, Natarajan V, Gaponenko V, & Mehta D (2020). SPHK2-generated S1P in CD11b+ macrophages blocks STING to suppress the inflammatory function of alveolar macrophages. Cell Reports, 30, 4096–4109. [PubMed: 32209471]
46. Üllen A, Fauler G, Bernhart E, Nusshold C, Reicher H, Leis HJ, Malle E, & Sattler W (2012). Phloretin ameliorates 2-chlorohexadecanal-mediated brain microvascular endothelial cell dysfunction in vitro. Free Radical Biology and Medicine, 53, 1770–1781. [PubMed: 22982051]
47. Usatyuk PV, & Natarajan V (2012). Hydroxyalkenal and oxidized phospholipids modulation of endothelial as cytoskeletal, focal adhesion, and adherens junction proteins in regulating endothelial barrier function. Microvasc Res, 83, 45–55. [PubMed: 21570987]
48. Zhang H, & Forman HJ (2017). 4-Hydroxynonenal-mediated signaling and aging. Free Radical Biology and Medicine, 111, 219–225. [PubMed: 27876535]
49. Chiarpotto E, Domenicotti C, Paola D, Vitali A, Nitti M, Pronzato MA, Biasi F, Cottalasso D, Marinari UM, Dragonetti A, Cesaro P, Isidoro C, & Poli G (1999). Regulation of rat hepatocyte protein kinase C beta isoenzymes by the lipid peroxidation product 4-hydroxy-2,3-nonenal: a signaling pathway to modulate vesicular transport of glycoproteins. Hepatology, 29, 1565–1572. [PubMed: 10216144]
50. Usatyuk PV, & Natarajan V (2004). Role of mitogen-activated protein kinases in 4-hydroxy-2-nonenal-induced actin remodeling and barrier function in endothelial cells. J Biol Chem, 279, 11789–11797. [PubMed: 14699126]
51. Negre-Salvayre A, Vieira O, Escargueil-Blanc I, & Salvayre R (2003). Oxidized LDL and 4-hydroxynonenal modulate tyrosine kinase receptor activity. Mol Aspects Med, 24, 251–261. [PubMed: 12893003]
52. Natarajan V, Scribner WM, & Taher MM (1993). 4-Hydroxynonenal, a metabolite of lipid peroxidation, activates phospholipase D in vascular endothelial cells. Free Radical Biology Medicine, 15, 365–375. [PubMed: 8225018]
53. Natarajan V, Scribner WM, & Vepa S (1997). Phosphatase inhibitors potentiate 4-hydroxynonenal-induced phospholipase D activation in vascular endothelial cells. Am J Respir Cell Mol Biol, 17, 251–259. [PubMed: 9271314]
54. Usatyuk PV, Parinandi NL, & Natarajan V (2006). Redox regulation of 4-hydroxy-2-nonenal-mediated endothelial barrier dysfunction by focal adhesion, adherens, and tight junction proteins. J Biol Chem, 281, 35554–35566. [PubMed: 16982627]
55. Chung F-L, Nath RL, Ocando I, Nishikawa A, & Zhang L (2000). Deoxyguanosine adducts of t-4-hydroxy-2-noneal are endogenous DNA lesions in rodents and humans: Detection and Potential Sources. Cancer Res, 60, 1507–1511. [PubMed: 10749113]
56. Galligan JJ, Rose KL, Beavers WN, Hill S, Tallman KA, Tansey WP, & Marnett LJ (2014). Stable histone adduct by 4-oxo-2-nonenal: A potential link between oxidative stress and epigenetics. J Am Chem Soc, 136, 11864–11866. [PubMed: 25099620]
57. Fu P, Ramchandran R, Sudhadevi T, Kumar PPK, Krishnan Y, Liu Y, Zhao Y, Parinandi NL, Harijith A, Sadoshima J & Natarajan V (2021). NOX4 mediates Pseudomonas aeruginosa-induced nuclear reactive oxygen species generation and chromatin remodeling in lung epithelium. Antioxidants (Basel), 10, 477. 10.3390/antiox10030477. [PubMed: 33802941]

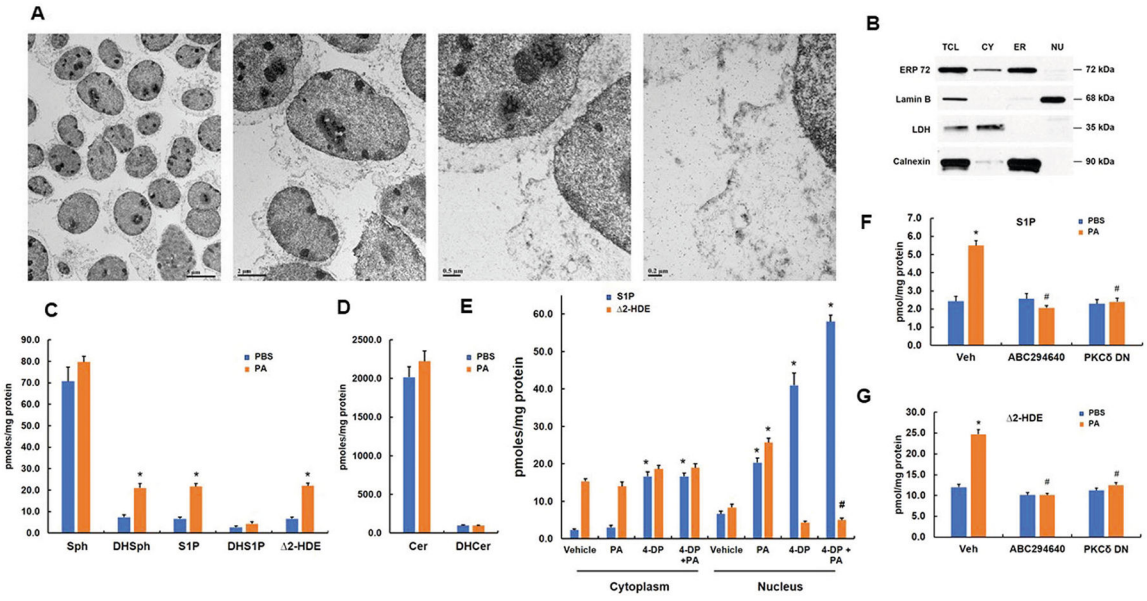

Fig. 1.

P. aeruginosa stimulates S1P and Δ2-hexadecenal in MLE-12 nuclear fraction. MLE-12 lung epithelial cells grown to ~90% confluence in 100-mm dishes were challenged with vehicle or heat-inactivated *P. aeruginosa* (PA, 1×10^8 CFU/ml) for 3 h. Cells were processed for isolation of cytosol, endoplasmic reticulum, and nuclear fractions as described in "Experimental Procedures" section using a detergent protocol followed by differential centrifugation. **A** The isolated nuclear fraction was subjected to TEM to determine purity of the nuclear fraction. No endoplasmic membrane contamination was found in the nuclear preparation. Shown is a representative TEM micrograph from several preparations. Scale bar—5 μm (×6000 magnification); Scale bar—2 μm (×50,000 magnification); Scale bar−0.5 μm (×75,000 magnification); and Scale bar—0.2 μm (×100,000 magnification). **B** Equal protein (~20 μg) from total cell lysate (TCL), cytosol (CY), crude endoplasmic reticulum (ER), and nuclear (NU) fractions were subjected to 10% SDS-PAGE and western blotting with specific primary and secondary antibodies: ER (ERP72 and Calnexin); cytosol (lactate dehydrogenase, LDH); Nuclear (lamin B). Shown is a representative blot from three independent experimental preparations. **C**, **D** Lipids were extracted from the nuclear fractions and levels of sphingosine (Sph), dihydrosphingosine (DHSph), ceramide (Cer), dihydroceramide (DHCer), sphingosine-1-phosphate (S1P), dihydrosphingosine-1-phosphate (DHS1P), and Δ2-hexadecenal (Δ2-HDE) were determined by LC-MS/MS and quantified. Values are means ± SEM of one experiment in triplicate and normalized to per mg protein. $*P < 0.05$, significantly different in *P. aeruginosa* treated cells compared to vehicle-treated cells. **E** MLE-12 lung epithelial cells grown to ~90% confluence in 100-mm dishes were preincubated with or without 4-deoxypyridoxine (4-DP, 10 mM) for 1 h prior to challenge with vehicle or heat-inactivated *P. aeruginosa* (PA, 1×10^8 CFU/ml) for 3 h. Cells were fractionated into cytosol, endoplasmic reticulum, and nuclear fractions as described in "Experimental Procedures" section using a detergent protocol followed by differential centrifugation. S1P and Δ2-HDE levels were determined by LC-MS/MS, quantified, and normalized to pmoles/mg protein. Values are mean ± SE from one

experiment in triplicate. *$P < 0.05$, significantly different in cells treated with 4-DP with or without *P. aeruginosa* challenge; #$P < 0.01$, significantly different in cells treated with 4-DP and *P. aeruginosa* compared to vehicle-treated cells. **F**, **G** MLE-12 lung epithelial cells grown to ~90% confluence in 100-mm dishes were transfected with vector control or adenoviral dominant-negative (DN) protein kinase C (PKC) δ adenoviral construct (10 MOI, 24 h) or preincubated with sphingosine kinase 2 (SPHK2) inhibitor ABC294640 (10 μM, 1 h) prior to challenge with vehicle or heat-inactivated *P. aeruginosa* (PA, 1×10^8 CFU/ml) for 3 h. Cells were fractionated into cytosol, endoplasmic reticulum and nuclear fractions as described in "Experimental Procedures" section using a detergent, and S1P and Δ2-HDE levels were determined by LC-MS/MS and quantified, and normalized to pmoles/mg protein. Values are mean ± SE from one experiment in triplicate. *$P < 0.05$, significantly different in cells challenged with *P. aeruginosa*; #$P < 0.001$, significantly different in cells treated with the SPHK2 inhibitor (ABC294640) or dominant-negative (DN) PKC δ adenoviral construct in cells challenged with *P. aeruginosa* compared to vehicle-treated cells

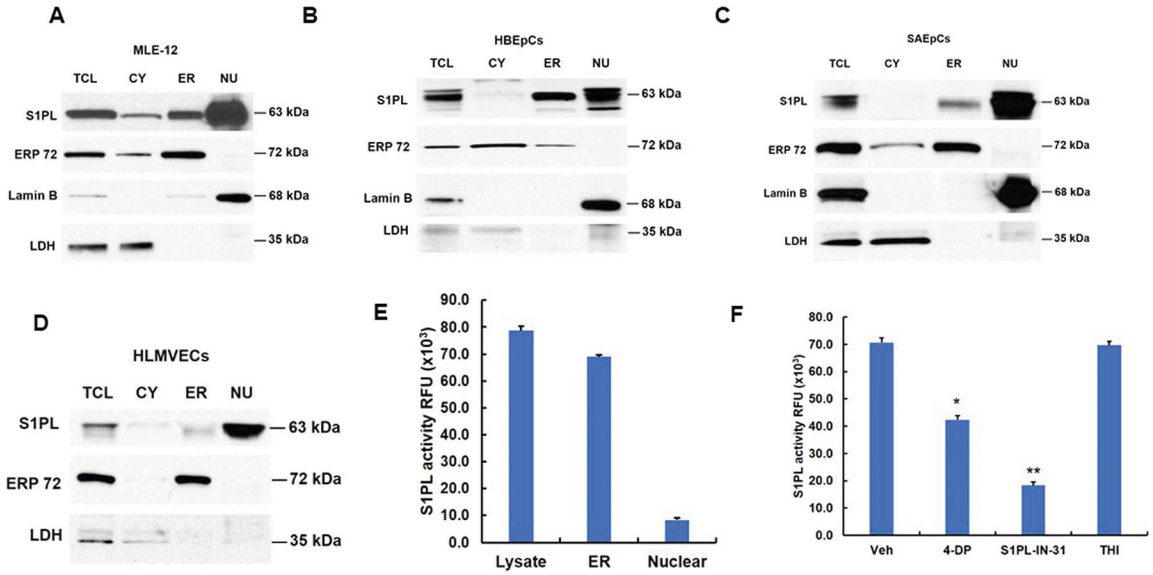

Fig. 2.

Expression and activity of S1P lyase in MLE-12 nuclear fraction-Nuclear fractions were prepared from MLE-12 lung epithelial cells (**A**), human bronchial epithelial cells (HBEpCs) (**B**), small airway epithelial cells (SAEpCs) (**C**), and human lung microvascular endothelial cells (HLMVECs) (**D**), and equal amounts of total protein (20 μg) were subjected to western blotting on 10% SDS-PAGE, and membranes were probed with anti-S1P lyase, anti-ERP72 (endoplasmic reticulum marker), anti-LDH (cytosol marker) or lamin B (nuclear marker) primary antibodies followed by appropriate secondary antibodies. Shown is a representative blot of several experiments. Localization of S1P lyase is clearly seen in the nuclear and endoplasmic fractions. (**E**), S1P lyase activity using the synthetic fluorogenic substrate and ~10–50 μg of protein, were used as outlined in "Experimental Procedures" section. The reaction was carried out for 30 min and the fluorescence of 7-hydroxycoumarin was measured in a spectrofluorometer. Values are means ± SE of three independent experiments in triplicate. (**F),** MLE-12 cells grown in 100-mm dishes were pretreated with vehicle, 4-deoxypyridoxine (10 mM) (a competitor of pyridoxal phosphate), S1PL-IN-31 (10 μM) (a small molecule inhibitor of S1P lyase) or THI (10 μM) (an inhibitor of S1P lyase that requires in vivo transformation to an active metabolite) for 2 h prior to isolation of the nuclear fraction as outlined in "Experimental Procedures" section. The nuclear fractions were dispersed in 25 mM HEPES buffer pH 7.4 containing 1% NP40 and assayed for S1P lyase activity as indicated in (**E**). Values are means ± SE of three independent experiments in triplicate, and S1P lyase activity represented as RFU ($x10^3$). *$P < 0.05$, significantly different in cells treated with 4-DP compared to vehicle; **$P < 0.001$, significantly different in cells treated with S1P lyase inhibitor, IN-31 compared to vehicle

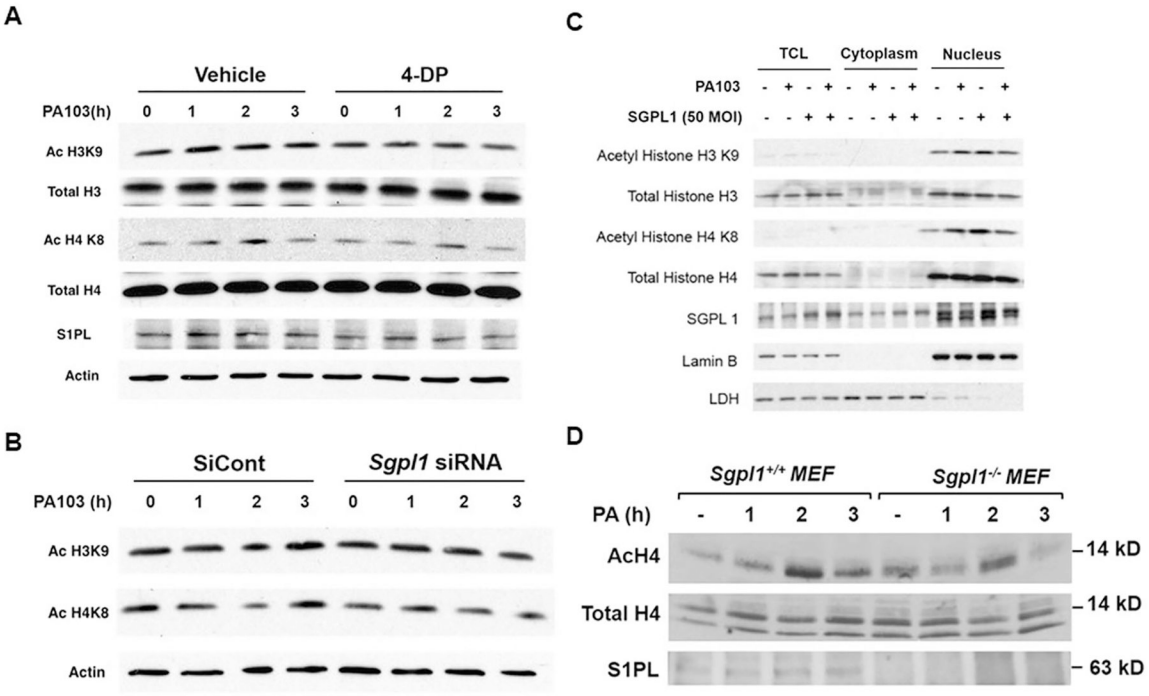

Fig. 3.

S1P lyase activity is essential for *P. aeruginosa*-mediated histone acetylation in MLE-12 lung epithelial cells-(**A**), MLE-12 lung epithelial cells grown in 100-mm dishes to ~90% confluence were pretreated with vehicle or vehicle + 4-DP (10 mM) for 1 h prior to challenge with heat-inactivated *P. aeruginosa* (1×10^8 CFU/ml) for 1, 2, and 3 h. Nuclear fractions were isolated as indicated in "Experimental Procedures" section, and reconstituted in cell lysis buffer. Nuclear lysates (20–30 μg protein) were subjected to 4–20% SDS-PAGE and immunoblotted with primary anti-AcH3K9, anti-AcH4K8, anti-S1P lyase, total H3, total H4 and total actin antibodies followed by appropriate secondary antibodies. Shown is a representative Western blot from three independent experiments. (**B**), MLE-12 lung epithelial cells grown in 100-mm dishes to ~60% confluence, were transfected with scrambled (scr) or S1P lyase (*Sgpl1*) siRNA (50 nM) for 48 h. The cells were challenged with *P. aeruginosa (*1×10^8CFU/ml) for 1, 2, and 3 h, nuclear fractions were isolated and nuclear lysates (20 μg protein) were subjected to 4–20% SDS-PAGE followed by immunoblotting with primary anti-AcH3K9, anti-AcH4K8 and anti-actin antibodies and appropriate secondary antibodies. Shown is a Western blot from three separate experiments. (**C**), MLE-12 lung epithelial cells grown in 100-mm dishes to confluence were infected with vector control or adenoviral $Sgpl1^{+/+}$ wild type (50 MOI) for 24 h. Cells were challenged with vehicle or *P. aeruginosa* for 3 h, cytoplasm and nuclear fractions were isolated, subjected to Western blotting (30 μg protein) on 4–20% SDS-PAGE and immunoblotted with primary anti-AcH3K9, anti-AcH4K8, S1P lyase (SGPL1), total H3, total H4, LDH and lamin B antibodies followed by appropriate secondary antibodies. Shown is a representative blot of one experiment in triplicate. **D** Mouse fetal lung fibroblasts (MEF) from wild-type and $Sgpl1^{-/-}$ mice grown in 100-mm dishes were challenged with heat-inactivated *P. aeruginosa* (1×10^8CFU/ml) for 1, 2, and 3 h, nuclear fractions were isolated and nuclear

lysates (30 μg protein) were subjected to 4–20% SDS-PAGE followed by Western blotting with primary anti-AcH4K8 (AcH4), anti-H4, and anti-S1P lyase (S1PL), and appropriate secondary antibodies. Shown is a representative blot from three independent experiments

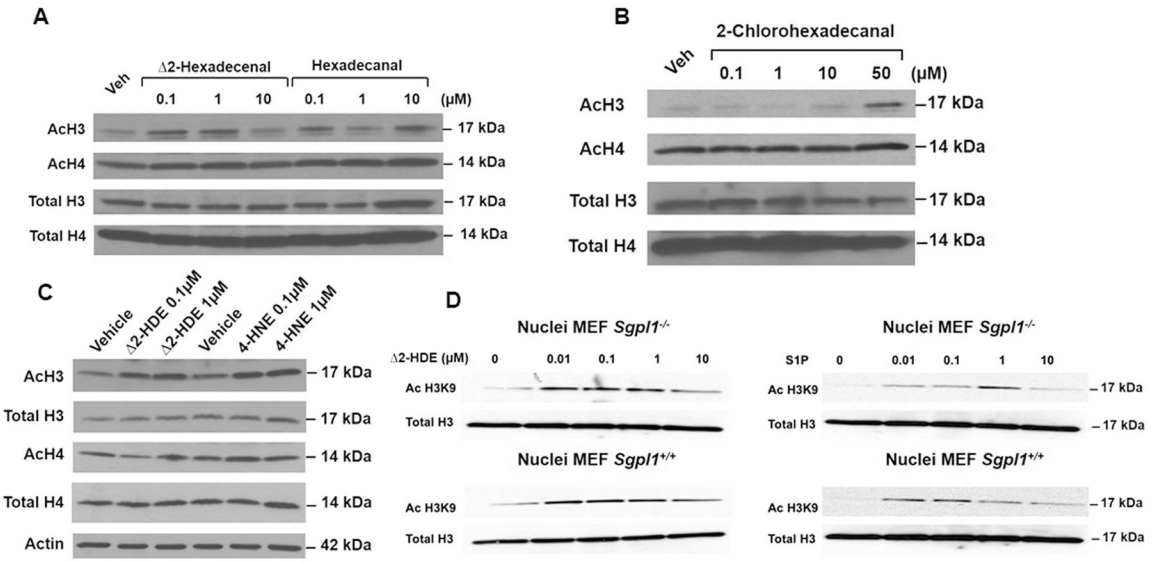

Fig. 4.

Δ2-Hexadecenal, but not S1P, stimulates histone acetylation in lung epithelial nuclear fraction-(**A**–**C**), nuclear fractions were isolated from MLE-12 lung epithelial cells grown in 100-mm dishes to ~90% confluence as described in “Experimental Procedures” section. Nuclear lysates (50 μg protein) were incubated with varying concentrations of (**A**), Δ2-hexadecenal (Δ2-HDE), hexadecanal, (**B**), 2-chlorohexadecanal, or (**C**), Δ2-HDE or 4-hydroxynonenal (4-HNE) for 30 min at 37 °C and were subjected to 4–20% SDS-PAGE and western blotting with primary anti-AcH3K9, anti-H4K8, anti-H3K9, anti-H4K8, and actin and appropriate secondary antibodies. Shown is a representative blot from three independent experiments. (**D**), Nuclear fractions from MEF (*Sgpl1*$^{+/+}$) and MEF (*Sgpl1*$^{-/-}$) cells (50 μg protein) were incubated with varying concentrations of Δ2-HDE (0.01–10 μM) or S1P (0.01–10 μM) for 30 min at 37 °C, and were subjected to 4–20% SDS-PAGE and Western blotting as described (**A**–**C**). Shown is a representative of three independent experiments

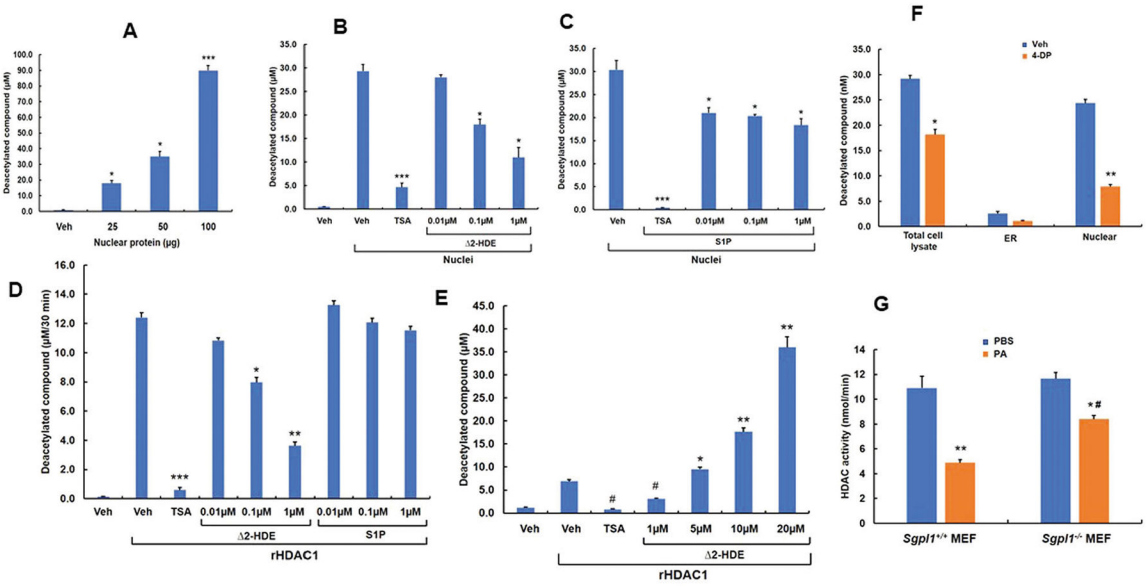

Fig. 5.

Δ2-Hexadecenal inhibits nuclear and recombinant HDAC1 activity in vitro-(**A**), HDAC activity in nuclear fractions isolated from MLE-12 cells (25–100 μg protein) was measured using 200 μM of acetylated fluorometric substrate in a final volume of 200 μl for 30 min at 37 °C as described in "Experimental Procedures" section. HDAC deacetylated standard curve was simultaneously run for quantitative determination of the HDAC activity in the nuclear fraction and expressed as deacetylated compound (μM) formed in 30 min. Values are means ± SE from triplicate samples. *$P < 0.05$, significantly different in nuclear fractions incubated with HDAC1 substrate; ***$P < 0.005$, significantly different in nuclear fractions incubated with HDAC1 substrate. (**B**), Δ2-Hexadecenal (Δ2-HDE) (0.01–1 μM) or trichostatin (TSA) (1 μM), was added to MLE-12 nuclear preparations (50 μg protein) in the presence of 200 μM of acetylated fluorometric substrate in a final volume of 200 μl for 30 min at 37 °C as described above. Values are means ± SE of duplicate experiments in triplicate. *$P < 0.05$, significantly different in nuclear fractions incubated with Δ2-HDE compared to vehicle without Δ2-HDE; ***$P < 0.005$, significantly different in nuclear fractions incubated trichostatin (TSA), a pan inhibitor of HDACs, compared to vehicle (**C**), Sphingosine-1-phosphate (S1P) of varying concentration (0.01–1 μM), sonicated in DMEM medium containing 0.1% bovine serum albumin was added to MLE-12 nuclear preparations (50 μg protein) and HDAC activity was monitored using 200 μM of acetylated fluorometric substrate and time as indicated above. Values are means ± SE of duplicate experiments in triplicate. *$P < 0.05$, significantly different in nuclear fractions incubated with S1P compared to vehicle-treated preparations. (**D**), Δ2-HDE (0.01–1 μM), S1P (0.01–1 μM) or trichostatin (TSA) (1 μM), was added to recombinant 100 nM HDAC1 in the assay buffer (25 mM Tris-HCl, pH 8.0, 137 mM NaCl, 2.7 mM KCl, and 1 mM $MgCl_2$), and the reaction was initiated by the addition of the 200 μM HDAC substrate in a final volume of 100 μl, and fluorescence was monitored as described in "Experimental Procedures" section. Values are means ± SE of one experiment in triplicate. *$P < 0.05$, significantly different in nuclear fractions incubated with Δ2-HDE compared to nuclear fractions without Δ2-HDE;

$^{**}P < 0.01$, significantly different in nuclear fractions incubated with Δ2-HDE compared to without Δ2-HDE; $^{***}P < 0.005$, significantly different in nuclear fractions incubated TSA, a pan inhibitor of HDACs. (**E**), Same as (**D**), but higher concentrations of Δ2-HDE (1–20 μM) were used with the rHDAC1 (100 nM) plus the acetylated fluorometric substrate (200 μM) for 30 min at 37 °C as indicated above. Values are means ± SE of one experiment in triplicate. $^{*}P < 0.05$, significantly different in nuclear fractions incubated with Δ2-HDE (5 μM) compared to vehicle without Δ2-HDE; $^{**}P < 0.01$, significantly different in nuclear fractions incubated with Δ2-HDE (10 and 20 μM) compared to vehicle without Δ2-HDE; $^{\#}P < 0.005$, significantly different in nuclear fractions incubated trichostatin (TSA), a pan inhibitor of HDACs compared to vehicle. **F** MLE-12 cells grown in 100-mm dishes to ~90% confluence, were treated with vehicle or vehicle containing 4-deoxypyridoxine (4-DP) (10 mM) for 2 h and trypsinized cells were subjected to nuclear preparation as indicated in "Experimental Procedures" section. The total cell lysates, endoplasmic reticulum fraction (ER) and nuclear fraction were incubated with acetylated fluorometric substrate (200 μM) in a final volume of 200 μl, fluorescence was monitored for 30 min, and deacetylated compound (μM) formed was quantified using the deacetylated compound standard curve as recommended by the HDAC activity kit manufacturer. Values are means ± SE of one experiment in triplicate. $^{*}P < 0.05$, significantly different in total cell lysates from 4-DP treated cells compared to vehicle without 4-DP; $^{***}P < 0.005$, significantly different in nuclear fractions isolated from 4-DP treated cells compared to vehicle without 4-DP; (**G**), wild-type MEF cells (*Sgpl1*$^{+/+}$) and *Sgpl1*$^{-/-}$ MEF cells in 100-mm dishes grown to ~90% confluence were challenged with vehicle or *P. aeruginosa* (*PA*) (1×10^8 CFU/ml) for 3 h. Nuclear fractions were isolated and HDAC1/2 activity in the nuclear fractions (50 μg protein) was measured using the acetylated fluorometric substrate (200 μM) in a final volume of 200 μl assay. HDAC activity was calculated using the deacetylated compound standard curve and represented as nmol/min. Values are means ± SE of one experiment in triplicate. $^{*}P < 0.05$, significantly different in nuclear fractions isolated from *Sgpl1*$^{-/-}$ MEF cells challenged with *P. aeruginosa* compared to vehicle-challenged cells; $^{**}P < 0.01$, significantly different in nuclear fractions isolated from *Sgpl1*$^{+/+}$ MEF cells challenged with *P. aeruginosa* compared to vehicle-challenged cells; $^{\#}P < 0.05$, significantly different in *P. aeruginosa*-challenged *Sgpl1*$^{-/-}$ MEF cells compared to *P. aeruginosa*-challenged *Sgpl1*$^{+/+}$cells

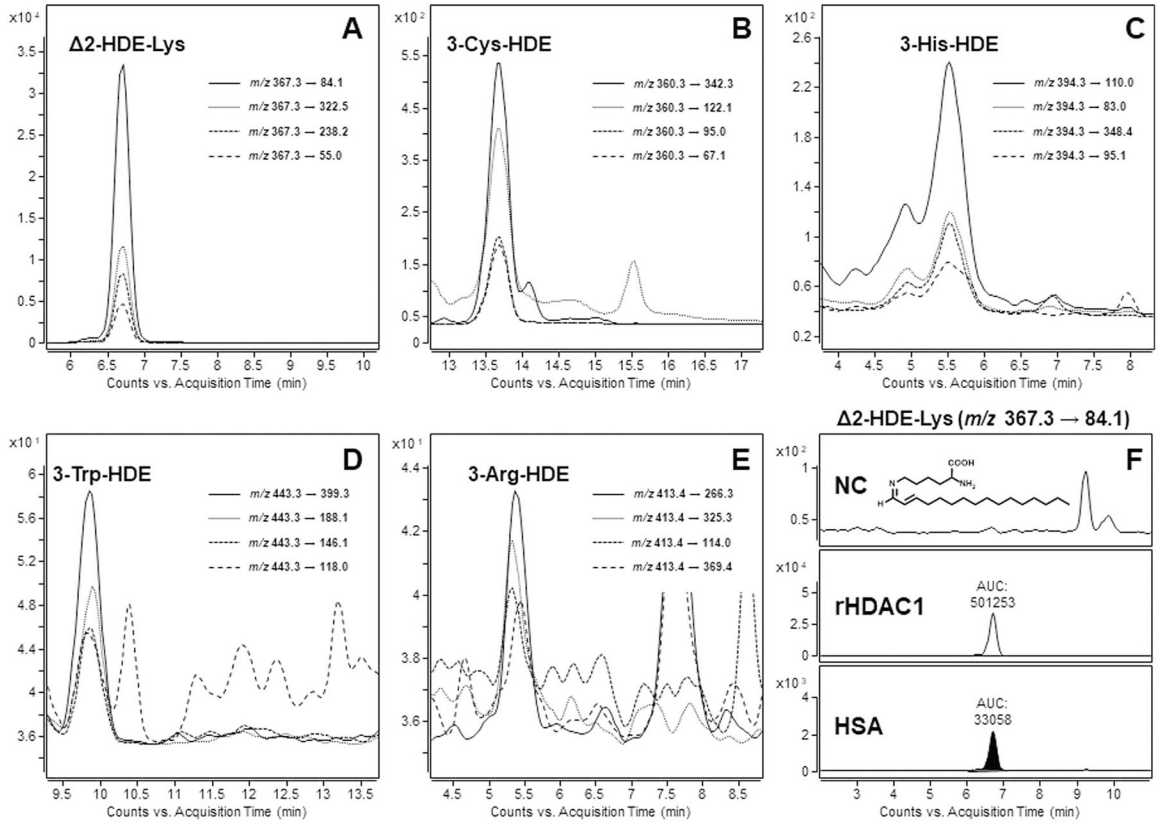

Fig. 6.

LC-MS/MS detection of in vitro generated protein adducts of Δ2-HDE with recombinant human HDAC1. After incubation of 50 μg rHDAC1 with 1 mM Δ2-HDE, the purified reaction mixture was subjected to enzymatic proteolysis and adducted amino acids were extracted and analyzed by LC-(ESI +)-MS/MS in multiple reaction monitoring (MRM) mode. A total of five different amino acid adducts were detected: a Schiff base (imine) product with lysine (**A**) and Michael addition products with cysteine (**B**), histidine (**C**), tryptophan (**D**), and arginine (**E**). Four mass transitions each (given as legends) were analyzed. The *y*-axes are scaled differently. **F** In parallel to rHDAC1, human serum albumin (HSA, positive control) and an approach without an initial protein source (negative control, NC) were processed analogously. An ~15-fold excess of the major adduct Δ2-HDE-Lys (chemical structure given as inset) was detected in rHDAC1 compared to HSA. A corresponding peak was missing in the NC.

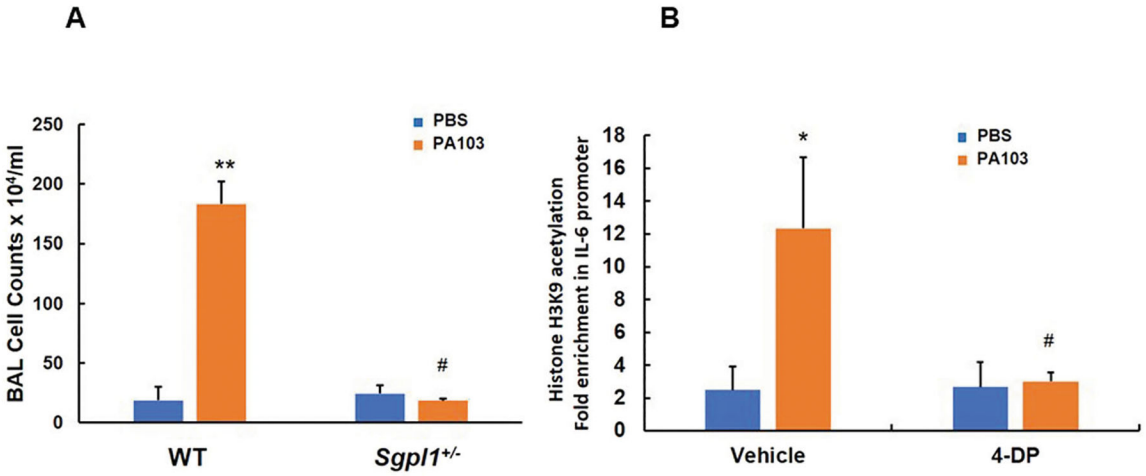

Fig. 7.

Partial deletion of S1P lyase (*Sgpl1*$^{+/-}$) in mice or inhibition of S1P lyase in MLE-12 cells attenuates *P.* aeruginosa-induced infiltration of inflammatory cells and IL-6 acetylation in the promoter-(**A**), 129/SV wild-type and *Sgpl1*$^{+/-}$ mice in same background were challenged intratracheally with sterile PBS or *P. aeruginosa* (1×10^6 CFU/mouse) for 24 h. Bronchoalveolar lavage (BAL) fluids from control and *P. aeruginosa*-challenged wild-type and *Sgpl1*$^{+/-}$ mice were collected and total infiltrated cells were counted using cytospin. Data are expressed as means ± SE from one experiment (number of animals per group = 3). $^{**}P < 0.01$, significantly different in wild-type mice exposed to *P. aeruginosa*; $^{\#}P < 0.001$, significantly different in *P. aeruginosa*-challenged *Sgpl1*$^{+/-}$ mice compared to *P. aeruginosa*-challenged wild-type mice. (**B**), MLE-12 cells grown in 100-mm dishes to ~90% confluence were pretreated with 10 mM 4-deoxypyridoxine (4-DP) for 1 h prior to challenge with vehicle or heat-inactivated *P. aeruginosa* (1×10^8 CFU/ml) for 3 h. Cell lysates (1 mg protein) were subjected to ChIP assay by immunoprecipitating acetylated H3K9 with ChIP grade anti-acetyl histone H3K9. The immunoprecipitates were analyzed by real-time quantitative PCR for NF-kB binding sites on IL-6 promoter. Values are means ± SE of one experiment in triplicate. $^{**}P < 0.05$, significantly different in MLE-12 cells exposed to *P. aeruginosa*; $^{\#}P < 0.001$, significantly different in MLE-12 cells treated with 4-deoxypyridoxine (10 mM) for 1 h prior to *P. aeruginosa* challenge compared to unchallenged cells

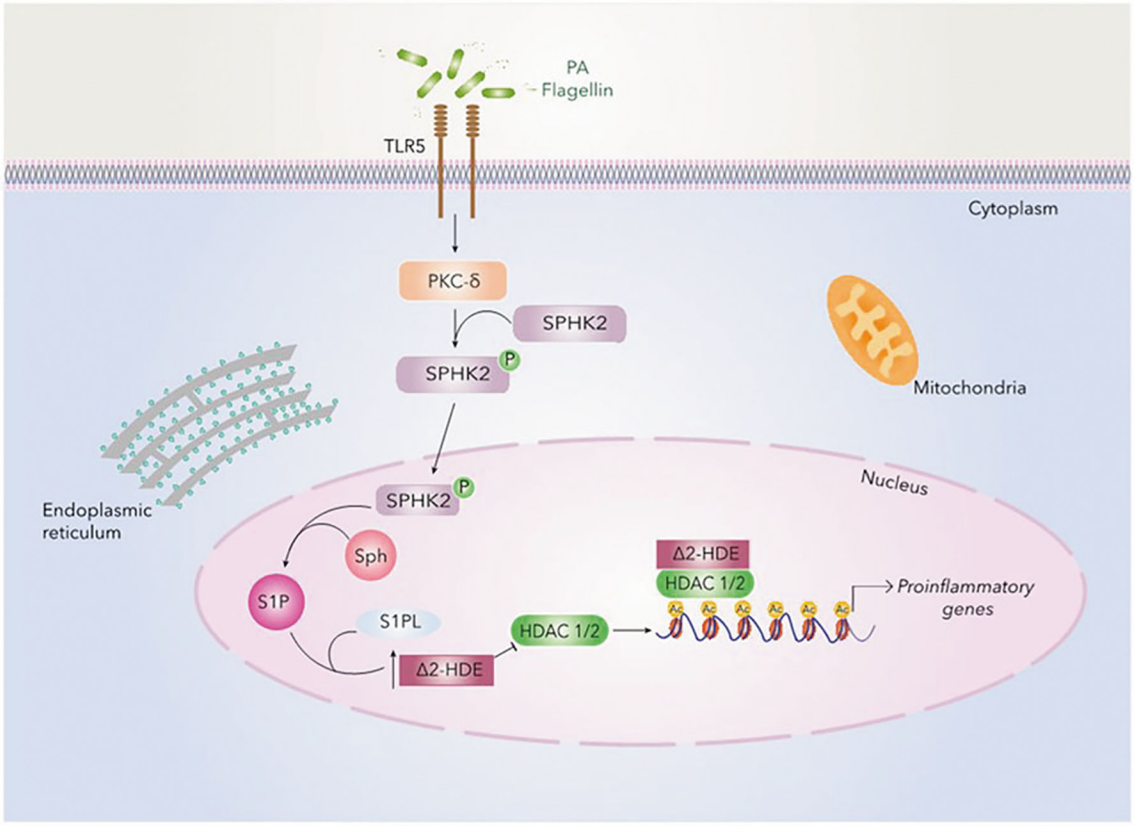

Fig. 8.

Inhibition of HDAC1/2 activity and chromatin remodeling by Δ2-hexadecenal generated from S1P by nuclear S1P lyase—*Pseudomonas aeruginosa* (PA) infection of mouse lungs or lung epithelial cells in culture enhances nuclear S1P via protein kinase C (PKC) δ mediated phosphorylation of sphingosine kinase (SPHK) 2 in the nucleus. The lung epithelial cell express S1P lyase (S1PL) in the nucleus in addition to endoplasmic reticulum (ER) and the nuclear S1P lyase hydrolyses the S1P generated to Δ2-hexadecenal (Δ2-HDE) and ethanolamine phosphate. Δ2-HDE forms Schiff base products (imine) with lysine and Michael adducts with cysteine, histidine, tryptophan. and arginine residues of HDAC1/2. Adducts in vitro with HDAC1/2 as shown in Fig. 6. However, the formation of Δ2-HDE adducts with HDAC1/2 in lung epithelial nuclei is yet to be demonstrated. Modification of HDAC1/2 by Δ2-HDE inhibits HDAC1/2 activity and prolongs the acetylation of H3 and H4 histones. Sustained acetylation of histones remodels the chromatin from a closed to open configuration that allows transcriptional factors, such as NF-kB to bind to promoter regions of pro-inflammatory genes and enhance gene expression. Thus, Δ2-HDE formed from S1P by S1P lyase localized in the nucleus can modulate HDAC1/2 activity and epigenetically regulate pro-inflammatory genes in lung epithelium and other cell types. ER endoplasmic reticulum